

1 **Neogene - Quaternary slow coastal uplift of Western Europe**
2 **through the perspective of sequences of strandlines from the**
3 **Cotentin Peninsula (Normandy, France)**

4

5 K. Pedoja^{1,2,3}, J. Jara-Muñoz⁴, G. De Gelder⁵, J. Robertson⁶, M. Meschis⁶, D.
6 Fernandez-Blanco⁵, M . Nexer^{1,2,3}, Y. Poprawski⁷, O. Dugué^{1,2,3}, B. Delcaillau^{1,2,3}, P.
7 Bessin⁸, M. Benabdelouahed^{9,10}, C.Authemayou^{9,10}, L.Husson^{11,12,13}, V.Regard^{14,15,16},
8 D. Menier^{9,10}, B. Pinel^{1,2,3}

9

10 ¹Normandie Univ, France ; ²UCBN, M2C, F-14000 Caen, France; ³CNRS, UMR 6143 M2C, F-14000
11 Caen, France kevin.pedoja@unicaen.fr. ⁴ Institut für Erd- und Umweltwissenschaften, University
12 Potsdam, 14476 Potsdam, Germany. ⁵Institut de Physique du Globe de Paris, Sorbonne Paris Cité,
13 Univ Paris Diderot, UMR 7154 CNRS, F-75005 Paris, France. ⁶Department of Earth and Planetary
14 Sciences, Birkbeck, University of London, WC1E 7HX, UK. ⁷Institute of Earth Sciences Jaume Almera,
15 ICTJA-CSIC, Group of Dynamics of the Lithosphere, Spain. ⁸LPG – Le Mans, UMR 6112, Université
16 du Maine, Avenue Olivier Messiaen, 72085 Le Mans, France. ⁹Laboratoire Domaines océaniques,
17 UMR 6538- IUEM, Université de Brest, CNRS, Plouzané, France. ¹⁰Université de Bretagne Sud,
18 GMGL IUEM CNRS 6538 Domaines Océaniques. ¹¹Univ. Grenoble Alpes, ISTerre, F-38014 Grenoble,
19 France ¹²CNRS, ISTerre, F-38014 Grenoble, France ¹³IRD, ISTerre, F-38014 Grenoble, France.
20 ¹⁴Université de Toulouse ; UPS (OMP) ; GET ; 14 Av Edouard Belin, F-31400 Toulouse, France ¹⁵
21 CNRS ; GET ; F-31400 Toulouse, France. ¹⁶IRD; GET ; F-31400 Toulouse, France.

22

Morpho-stratigraphy of low-lying terraces from N Cotentin

Description of the polygenic coastal erosion surfaces (rasas) of Cotentin

Late Cenozoic paleogeographic evolution

Database on Neogene and Quaternary shorelines of Western Europe

Wholesale analysis of the Late Cenozoic uplift of Western European coastlines

23 **Keywords** : marine terrace; rasa; Cotentin and western Europe; Neogene and
24 Quaternary coastal uplift

25

26 **Abstract**

27

28 The Cotentin Peninsula (Normandy, France) displays sequences of marine terraces
29 and rasas, the latter being wide Late Cenozoic coastal erosion surfaces, that are
30 typical of Western European coasts in Portugal, Spain, France and southern
31 England. Remote sensing imagery and field mapping enabled reappraisal of the
32 Cotentin coastal sequences. From bottom to top, the N Cotentin sequence includes
33 four previously recognized Pleistocene marine terraces (T1 to T4) at elevations < 40
34 m as well as four higher and older rasas (R1 to R4) reaching 200 ± 5 m in elevation.
35 Low-standing marine terraces are not observed in the central part of the Peninsula
36 and a limited number of terraces are described to the south. The high-standing rasas
37 are widespread all over the peninsula. Such strandline distributions reveal major
38 changes during the Late Cenozoic. Progressive uplift of an irregular sea-floor led to
39 subaerial exposure of bathymetric highs that were carved into rocky platforms, rasas
40 and marine terraces. Eventually, five main islands coalesced and connected to the
41 mainland to the south to form the Cotentin Peninsula. On the basis of previous dating
42 of the last interglacial maximum terrace (i.e. Marine Isotopic Stage, MIS 5e),
43 sequential morphostratigraphy and modelling, we have reappraised uplift rates and

44 derived: (i) mean Upper Pleistocene (i.e. since MIS 5e ~ 122 +/- 6 ka, i.e. kilo annum)
45 apparent uplift rates of 0.04 ± 0.01 mm/yr, (ii) mean Middle Pleistocene eustasy-
46 corrected uplift rates of 0.09 ± 0.03 mm/yr, and (iii) low mean Pleistocene uplift rates
47 of 0.01 mm/yr. Extrapolations of these slow rates combined with geological evidence
48 implies that the formation of the sequences from the Cotentin Peninsula occurred
49 between 3 Ma (Pliocene) and 15 Ma (Miocene), which cannot be narrowed down
50 further without additional research. Along the coasts of Western Europe, sequences
51 of marine terraces and rasas are widespread (169 preserve the MIS 5e benchmark).
52 In Spain, Portugal, S England and other parts of western France, the sequences
53 morphostratigraphy is very similar to that of Cotentin. The onset of such Western
54 European sequences occurred during the Miocene (e.g. Spain) or Pliocene (e.g.
55 Portugal). We interpret this Neogene - Quaternary coastal uplift as a symptom of the
56 increasing lithospheric compression that accompanies Cenozoic orogenies.

57

58 **1 Introduction**

59

60 Emerged sequences of fossil coastal landforms (marine terraces and rasas which are
61 wide Late Cenozoic polygenic coastal platforms) with associated deposits ("raised
62 beaches") are present along the shores of Western Europe, in Portugal, Spain,
63 France, UK and Ireland (Pedoja et al., 2011; 2014). In France and in the British Isles,
64 earlier studies (e.g., Prestwich, 1862-1863, 1892; Home, 1912; Coutard et al., 2006) -

65 with notable exceptions (e.g., Guilcher 1974; Lautridou, 1989) - ignored the higher
66 and older landforms (i.e. the rasas) within the coastal sequences, while in Iberia,
67 rasas were long interpreted as geomorphic indicators of former sea levels (e.g.,
68 Breuil et al., 1942; Teixeira, 1944).

69

70 Herein, we reappraise the coastal sequences of the Cotentin Peninsula (Normandy,
71 France) because this area exhibits some of the northernmost long-lasting (i.e.
72 including rasa) coastal sequences along the Atlantic passive margin where
73 Pleistocene coastal deformation is generally homogeneous over long distances
74 (Pedoja et al., 2014). We mapped the Neogene and Quaternary strandlines from
75 Cotentin and measured their elevations through field studies, satellite images
76 (*Landsat, SPOT*) and Digital Elevation models DEM (MNT *Litto 3D* provided by *IGN*,
77 Institut de Géographie National). Age controls come from previous studies at the
78 same sites (e.g., Antoine et al., 1998; Cliquet et al., 2003; 2009; Coutard, 2003;
79 Coutard et al., 2005, 2006, Clet-Pellerin et al., 1997; van Vliet-Lanoë et al., 2002;
80 Dugué, 2003). We derived and extrapolated different Pleistocene uplift rates and
81 undertook modelling to propose plausible age ranges for the undated strandlines of
82 the sequence. The inferred timing is then discussed within the broader framework of
83 regional geology. The Late Cenozoic paleogeographical evolution of Cotentin has
84 already been interpreted as that of an island that connected to the mainland (see van
85 Vliet-Lanoë et al., 2000; 2002). We present geomorphic evidence – the pattern of
86 fossil shorelines associated with the rasas – which support this evolution.

87

88 In order to reframe the uplift of the Cotentin Peninsula and to evidence coastal uplift
89 at a continental scale, we compiled a regional synthesis of Late Cenozoic sea-level
90 changes for Atlantic Europe (Portugal, Spain, France, and the British Isles). The
91 coastal sequences of Western Europe have been somehow neglected in the most
92 recent global approaches (e.g. Murray-Wallace and Woodroffe, 2014; Pedoja et al.,
93 2014) and not interpreted as a continuous, 2000 -km-long uplifted coastal segment.

94

95 **2 Settings**

96

97 **2.1 Geodynamics and geology**

98

99 Since the upper Cretaceous, the convergence between the African and the European
100 plates affected the Western European passive margin. During the Pyrenees and the
101 Alpine orogenies, the main compressive stages reactivated structures of the passive
102 margin from upper Cretaceous to lower Miocene (e.g., Dèzes et al., 2004) with high
103 convergence rates, (~ 20 mm/yr) during the upper Cretaceous (Rosenbaum et al.,
104 2002). From the Late Miocene to the Quaternary, the convergence is characterized
105 by low rates with a modern rate ranging from 2 to 5 mm/yr (Dèzes et al., 2004). In the

106 foreland, convergence coincided with oblique extensional processes such as the
107 opening of the European Cenozoic rifts (Dèzes et al., 2004).

108

109 The Cotentin Peninsula on the North Atlantic margin, forms a promontory into the
110 English Channel (Fig. 1). The Peninsula belongs to the Armorican Massif and bounds
111 the Paris Basin (Juignet, 1980). Its basement, into which the marine terraces and
112 rasas are carved, is made of sedimentary and igneous rocks (Dupret et al., 1990;
113 Ziegler and Dèzes, 2007; Ballèvre et al., 2009). Cadomian and Variscan faults delimit
114 N 70° and N 120° grabens on the peninsula (Gresselin, 2000; Butaeye, 2001;
115 Lagarde et al. 2000; 2003). During the second half of the Mesozoic, the Peninsula
116 emerged and continental erosion/subtropical alteration induced the planation of the
117 Variscan topography (Klein, 1975), although Cenomanian marine incursions are
118 known (Dugué et al., 2007; 2009; Bessin, 2015). During the Cenozoic, compressive
119 events alternated with relaxation phases (van Vliet-Lanoë et al., 2002); the Peninsula
120 was exposed to alternating marine sedimentation (coming from the west) and
121 continentalisation (Guilcher, 1949; Klein, 1975; Baize, 1998; Bonnet et al., 2000; van
122 Vliet-Lanoë et al., 2002; Guillocheau et al., 2003; Dugué et al., 2007, 2009; Bessin et
123 al., 2015). On the NW Armorican massif, Paleogene long wavelength/low amplitude
124 deformation (Dugué, 2003; Dugué et al. 2007, 2009) resulted in uplift, emergence,
125 and subtropical subaerial weathering of the area which led to the formation of a
126 planation surface (Baize, 1998; Ziegler, and Dèzes, 2007). During the late Middle
127 Eocene, the North Atlantic waters reoccupied the area (Dugué, 2003; Dugué et al.,

128 2007, 2009; Bauer et al., 2016). Upper Eocene and Lower Oligocene deformations of
129 the area (Bonnet et al., 2000; Guillocheau et al., 2003; Dugué, 2003; Dugué et al.,
130 2007; 2009) induced a resurfacing of the main planation surface to a lower one.
131 North Cotentin emerged during the Upper Paleocene (Dugué et al., 2009), whereas
132 in the Seuil du Cotentin basin (Fig. 1C), marine incursions occurred during the
133 Oligocene and Middle Miocene times (Langhian – Serravallian, open marine facies;
134 Baize, 1998; van Vliet-Lanoë et al., 2002; Dugué et al., 2009). As the closure of the
135 seaway once constituted by the Seuil du Cotentin area is an important benchmark for
136 the regional coastal evolution, its Plio-Quaternary sedimentary record is presented
137 and discussed section 4.4.3.

138

139 **2.2 Geomorphology**

140

141 The English Channel bordering the Cotentin Peninsula is an epi-continental sea; its
142 floor, presently at <60 m, emerged periodically over glacial cycle timescales. During
143 low-stands, the sea bottom was dissected by a fluvial network that constitutes, at
144 present, the offshore extension of modern rivers (the Seine, the Somme and the
145 Solent) (Graindor, 1964; Larsonneur et al., 1975; Auffret et al., 1980; Gibbard, 1988;
146 Hamblin et al., 1992; Bridgland, 2002; Antoine et al., 2003; Lericolais et al., 2003;
147 Mellett et al., 2013; Tessier et al., 2013). These rivers acted as tributaries that

148 merged during glacial low-stands into a larger river positioned off the present coast of
149 Cotentin (Larsonneur et al., 1975; Benabdellouahed, 2013).

150

151 The coasts of Cotentin are characterized by sea-cliffs with elevations of ~ 100 m at
152 Nez de Jobourg and less than ~ 4 m near Dielette (Fig. 1C). The cliffs alternate with
153 sedimentary embayments underlined by pebble or shingle beaches and/or beach-
154 ridges lying on sand (e.g. Ecalgrain embayment). At many sites, Quaternary
155 continental deposits such as Holocene dunes or Pleistocene loess and periglacial
156 deposits, known as heads, are overlying the terraces (i.e. Biville and Hatainville area,
157 West Cotentin, North of Barneville-Carteret) (Lautridou et al., 1999).

158

159 The raised beaches and marine terraces from Cotentin have been extensively
160 studied over 120 years (e.g., Bigot, 1897, 1898, 1930, 1931; Elhaï, 1960; Graindor,
161 1964; Pareyn, 1980; Scuvée and Alduc, 1981; Lautridou, 1983, 1985, 1989;
162 Lautridou et al., 1999; Coutard, 2003; Coutard et al., 2005, 2006; Cliquet et al., 2009;
163 Cliquet, 2015; Nexer, 2015). To the NE of the Peninsula (Fig. 1C), Coutard et al.,
164 (2006) described four terraces culminating at ~40 m; T1 has its shoreline angle (i.e.
165 the intersection between the rocky platform and the fossil sea cliff of a marine
166 terrace) at 6 ± 1 m NGF (the Principal Datum for France, Nivellement général de la
167 France, see definition NGF section 3), T2's shoreline angle was measured at 17 ± 2
168 m NGF. The shoreline of T3 is present at 26 ± 2 m, and that of T4 at 31 ± 2 m, locally

169 at 38 ± 1 m (Coutard et al., 2005, 2006). Based on five luminescence (OSL) datings
170 on T1 coastal deposits sampled at the inner edge of the T1 terrace, Coutard et al.
171 (2006) proposed to allocate T1 to T4 to the last four interglacials (MIS 5e, 7, 9, and
172 11). A submerged terrace, observed on bathymetrical charts at –20 m NGF at La
173 Mondrée site (LM on Fig. 1C) was interpreted as the geomorphic record of a sea-
174 level stand during Marine Isotopic Stage (MIS) 5c or 5a (Coutard et al. 2006). Later
175 studies focused on archaeology and environmental settings (e.g. Cliquet & Lautridou,
176 2009) using luminescence dating of the Middle Palaeolithic settlements at Gélétan,
177 Anse du Brick, Port-Racine, Ecalgrain bay, and Le Rozel sites (Cliquet et al., 2003,
178 2009; Cliquet, 2015). MIS 7 deposits were described on T2 at Rocher Gélétan and
179 on T1 on the North Ecalgrain Bay. The dating performed at Rocher Géletan was
180 carried out on reworked burnt flint (*silex chauffé en position secondaire*, Cliquet et al.,
181 2003) and impedes a confident correlation with MIS 7. At the Ecalgrain site, MIS 7
182 deposits have been described below those related to MIS 5e (Lautridou, 1983). A
183 more recent study, including dating, proposed a reworking by periglacial processes of
184 the MIS 7 coastal deposits on the MIS 5e platform (Cliquet et al., 2009).

185

186 Less attention has been paid to the coastal sequences of S Cotentin (Fig. 1B). To the
187 SW, at sites Hacqueville and Hauteville-Annoville (sites 9 and 10 on Fig. 1B), the MIS
188 5e benchmark defines a strandline conforming to the modern one (Lautridou 1983,
189 1985, 1989; Lautridou et al., 1999). To the SE of the Seuil du Cotentin, a sequence
190 of marine terraces is described at Grandcamp Maisy (site 19 on Fig. 1B; Lautridou,

191 1989; Coutard et al., 1979; Coutard and Lautridou, 1975), Asnelle Meuvaine (site 20
192 Fig. 1B; Bates et al., 2003; Pellerin et al., 1987) and Graye (site 21 Fig. 1B; Pellerin
193 and Dupeuble, 1979).

194

195 Concerning the upper part of the sequence, marine deposits on the La Pernelle
196 platform (NE Cotentin) were described at 90-110 m (Pareyn, 1980) but the outcrops
197 were not further observed (Baize, 1998). The sediments described (Pareyn, 1980)
198 are undated, azoic, supposedly marine deposits present at La Pernelle but also on
199 the rasa south of Cherbourg (Hameau du Cloquant, La Glacerie, on La Boissais fossil
200 island, see below) (Vérague, 1983). For the latter site, Vérague (1983) did a
201 granulometric and chemical comparison with deposits from another outcrop in the
202 area, and proposed a pre-Pliocene age for those deposits. Vérague (1983) noted
203 that: i) their morphometric parameters are different from those of Cenomanian and
204 Quaternary deposits, and, ii) their high kaolinite-content and depletion in silica
205 suggests weathering under subtropical climates. In NE Cotentin, Coutard et al.
206 (2006) described the lower part of the coastal sequence as overlooked by several
207 high "continental plateaux" ranging from 90 to 150 m (Coutard et al., 2006). Bessin et
208 al. (2015) also interpreted the upper surfaces of N Cotentin as continental in origin. In
209 S Cotentin, Lautridou (1989) described Pliocene and Miocene coastal deposits
210 ("Walton Crag") within the same area, to the NE of Hauteville-Annoville (site 10 Fig.
211 1B). Lautridou (1989) highlighted the relationship between the deposits and planation
212 surfaces (that he named plateaux). Describing two planation surfaces (called rasas in

213 this study) with Miocene and Pliocene deposits, he concluded that the platforms were
214 not separated by faults which could be explained by their marine origin. Finally, 120
215 km southward of N Cotentin, in the Mayenne area (site Champéon and Saint-Denis–
216 de-Gastines in Table 3 supplementary data), some outcrops are interpreted as
217 Pliocene coastal deposits (which reworked older Cenomanian to Eocene deposits)
218 overlying marine planation surfaces (i.e. rasas) (Gautier, 1967; Fleury et al., 1989).
219 We emphasize that the rasas possibly reshaped antecedent continental planation
220 surfaces, as some of them are overlain by scattered marine sedimentary remnants
221 (see Bessin et al., 2015 for a review).

222

223 **3 Background and methods**

224

225 **3.1 Late Cenozoic coastal staircase sequences and sea level**

226

227 Late Cenozoic staircase sequences of coastal indicators develop concomitantly with
228 sea-level changes on uplifting coastlines (Lajoie, 1986; Murray-Wallace and
229 Woodroffe, 2014). The elevation of the shoreline angle (i.e. intersection between the
230 rocky platform and the fossil sea cliff) of a marine terrace or a rasa (see below for
231 definitions) provides a good approximation to the location and elevation of a former
232 shoreline and, hence, a marker for relative sea level (Lajoie, 1986). The sequence

233 corresponds to the geomorphic record of the Late Cenozoic high-stands (interglacial
234 and interstadial) superimposed on an uplifting coast (Lajoie, 1986). At a global scale
235 the formation of coastal sequences was likely operative since minima in the middle
236 Miocene and locally (regionally) since the Eocene. The staircase shaping of coasts
237 increased during the Pliocene and Pleistocene as a consequence of the
238 intensification of eustatic sea-level oscillations (Pedoja et al., 2014), as inferred from
239 the isotopic record (Lisiecki and Raymo, 2005).

240

241 **3.2 Description of landforms**

242

243 As rocky shore platforms, their modern counterpart, *marine terraces* are flat coastal
244 surfaces bounded by steeper slopes, the inner slopes corresponding to a fossil sea
245 cliff (Bradley, 1957; Bradley and Griggs, 1976; Lajoie, 1986). Marine terraces form as
246 a result of coastal erosion ("wave-cut" terraces, i.e. a fossil rocky shore platform as in
247 Bradley, 1957) combined with accumulation of shallow marine deposits (Murray
248 Wallace and Woodroffe, 2014). Depending on the thickness of the coastal deposits
249 on the fossil shore platform (more or less than 1-2 m) there is a distinction between a
250 marine terrace and a wave-built terrace (Jara-Muñoz & Melnick, 2015). "Raised
251 beaches" is old terminology (Dunlop, 1893) that corresponds to the coastal deposits
252 associated with a marine terrace found emerged within the sea cliff and generally
253 overlain by continental deposits. The *shoreline angle* of a terrace (or a rasa – see

254 below) corresponds to the intersection between the fossil coastal platform and the
255 fossil sea cliff. Its elevation is used in any quantification of tectonics or eustatic sea
256 level (Lajoie, 1986).

257

258 *Rasas* are wide, elevated coastal planation surfaces corresponding to sequences of
259 terraces wherein the shoreline angles are not observed. (see Fig. 2 in Pedoja et al.
260 2014). The word “rasa”, first used to describe such rocky surfaces on the northern
261 coasts of Spain (Cueto and Rui Diaz, 1930; Hernandez-Pacheco 1950 both in
262 Guilcher, 1974), was extended to landforms present in Morocco (e.g. Oliva, 1977),
263 Tunisia (Paskoff and Sanlaville, 1983), Algeria (Authemayou et al., 2017), Lebanon
264 (Sanlaville, 1974), Chile (e.g. Regard et al., 2010; Melnick, 2016), Peru and Ecuador
265 (where rasa are locally named Tablazo e.g. Sheppard, 1927; 1930; Pedoja et al.
266 2006a, b), Costa Rica (Battistini and Bergoeing, 1982), eastern Canada (Allard and
267 Tramblay, 1981) and Scotland (Dawson et al., 2013). Rasas are: 1) of polygenic
268 origin - marine erosion occurred during various stands in sea level suggesting that re-
269 occupation processes occurred on the rocky platform (Pedoja et al. 2006a,b; 2011;
270 2014; Regard et al. 2010; Dawson et al., 2013; Melnick, 2016; Authemayou et al.,
271 2017); and 2) old features, as evidenced through direct dating; i.e. >0.5 Ma (e.g.,
272 Alvarez-Maron et al., 2008; Quezada et al., 2007) and most generally associated to
273 areas experiencing low uplift (< 0.2 mm/yr; Pedoja et al. 2011, 2014; Melnick, 2016; ;
274 Authemayou et al., 2017). In short, on slowly uplifting coasts, the formation of rasas
275 was promoted before and during early Pleistocene times, during periods of faster

276 oscillations and lower amplitudes in sea-level fluctuations than since the Middle
277 Pleistocene.

278

279 Fig. 2 sketches a 3D idealized view of a coastal sequence similar to that of Cotentin
280 which extends above sea level (rasa 1 to 4, Terrace T1 to 4), at sea level (T0 the
281 modern shore platform) and below sea level (T -1). The terraces and rasas are
282 defined as sub-planar, shallowly seaward-dipping surfaces between sea cliffs. T3 is
283 a compound terrace; it locally includes a low fossil sea cliff (< 2 m) separating two
284 terraces (T3' and T3" on Fig. 2). Marine cliffs are ~ 2 – 50 m high, and show two
285 fossil islands (Fig. 2A). Depending on the paleogeography, uplift rates and the
286 conservation of the landforms, the number of successive terraces observed in the
287 landscape at a given point can vary drastically. The maximum number of emerged
288 successive shorelines is 9 (not represented) including T3" and T3' (as on Transect
289 IV, Fig. 2C) but on transect III and V this number is reduced to 2 and 3, respectively.

290

291 **3.3 Mapping**

292

293 High-resolution topography (LiDAR) and surface classification models were used to
294 isolate remnants of marine terraces and rasas (Bowless and Cowgill, 2012). We used
295 swath profiles and semi-automated mapping of the surfaces associated with the

296 marine terraces and rasas using 5 -m-resolution topography (DEM Litto 3D, details in
297 Nixer, 2015) combined with morphometric analysis. We developed a Surface
298 Classification Model (SCM) to recognize terraced levels, as in Bowless and Cowgill
299 (2012). Inputs into the model are the topographic slope and roughness, calculated
300 herein as in Burrough and McDonnell (1998) and Frankel and Dolan (2007), using a
301 15x15 m roving-window (Fig. 3 A - D). The surface roughness is regarded as the
302 standard deviation of slope of cells within the roving-window. Both topographic
303 parameters were clipped from histograms (Fig. 3 E and F), using 90% of the
304 distributions (15° slope and 4 roughness). The values above these thresholds,
305 represented by gullies, valley slopes, and cliffs, are then removed to isolate the flat
306 and smoothed surfaces characteristic of rasas and marine terraces (Fig. 3 B - D).
307 Both truncated distributions were combined and normalized using a lineal equation
308 (Eq. 1) to create the SCM.

309

310
$$\text{SCM} = (\text{SLP} / \text{SLP_range}) * 0.5 + (\text{RGH} / \text{RGH_range}) * 0.5 \quad (\text{Eq. 1})$$

311

312 where SLP and RGH are the surface slope and roughness, and SLP_range and
313 RGH_range are the thresholds used to clip the topographic parameters. Then, the
314 SCM was intersected with the topography to obtain elevation distributions studied
315 using histograms and along profile projections. Marine terraces and rasas were
316 isolated through elevation bands in histograms (Fig. 3, 4B-C), where the limits of

317 these bands in histograms represent their inner and outer edges (Bowless and
318 Cowgill, 2012).

319 Swath profiles were extracted perpendicular to terrace edges using TerraceM®
320 (Jara-Muñoz et al., 2016); the maximum distribution of elevations on swaths was
321 used to estimate the inner-edge (shoreline angle) elevations and for displaying the
322 elevation patterns of rasa levels identified by the SCM.

323

324 **3.4 Measurements of elevations**

325

326 We focused our field efforts on North Cotentin. There, as elsewhere, the elevations of
327 coastal landforms should be measured with reference to their modern counterparts,
328 instead of in relation to a hydrological sea level which corresponds to the Principal
329 Datum, characteristic of each country (Jardine, 1981; van de Plassche, 1986). The
330 hydrographic sea level in France (NFG, IGN-1969, Nivellement Général de la France
331 made by Institut Géographique National in 1969) is not sufficiently accurate for the
332 Cotentin Peninsula (see Coutard, 2003; Nexer, 2015). Consequently, for the
333 measurements of elevation from barometrical altimeters, we generally tied the
334 elevation measurements to the modern shoreline angle (break of slope between the
335 modern platform and the sea cliff) that correspond to the *morphological* sea level and
336 performed repeated measurements. We also measured the elevations of shoreline
337 angles with differential GPS (Global Positioning System), also repeatedly when

338 possible. We used a Trimble Geoexplorer 2008 (horizontal and vertical precision of 1
339 m) and we made our measurements according to the French P.D. that was also tied
340 to the morphological sea level (Table 1). The Cotentin Peninsula area is macro-tidal
341 and we assume that the tide range remained steady through the period of time
342 covered by our study even if changes in coastal paleogeography such as those
343 evidenced herein may have induced changes in tidal amplitudes. We assigned an
344 error to each measurement depending on the preservation of fossil shorelines. These
345 errors increase with the elevation and degradation of the coastal indicators, from 1-
346 2 m for the low-standing terraces to up to 10 m for the uppermost rasa.

347

348 **3.5 Sea-level curves used and uplift rates**

349

350 Several Quaternary sea-level curves have been derived from the isotopic and/or
351 geomorphic records (Waelbroeck et al., 2002; Lisiecki and Raymo, 2005; Siddall et
352 al., 2006; Zachos et al., 2008; Bintanja and Van de Waal, 2008; Rohling et al., 2009;
353 Murray-Wallace and Woodroffe, 2014). For each MIS, the sea-level curves vary by
354 several thousand years (ka) in age and by several metres in height, that collectively
355 yield some inaccuracies when used (Caputo, 2007). Nevertheless, there is relative
356 consensus on the succession and ages of the most recent high-stands.

357

358 The most commonly investigated high-stand in the geomorphological record is the
359 last interglacial period allocated to MIS 5 (e.g., Stirling et al., 1998; Murray-Wallace
360 and Woodroffe, 2014), and which includes three relative high-stands, MIS 5a (85 ± 5
361 ka), MIS 5c (105 ± 5 ka) and MIS 5e (128 ka to 116 ka). MIS 7 ranges from 190 to
362 245 ka (Thompson and Goldstein, 2005), and includes sub-stages 7a, 7c and 7e
363 (Dutton et al., 2009). Two sea-level high-stands occurred within MIS 9, sub-stages 9a
364 and 9c extending from 306 ± 3 ka to 334 ± 4 ka respectively ($\sim 324.5 \pm 18.5$ ka;
365 Stirling et al., 2001). MIS 11 lasted from 420 ka to 360 ka (Murray Wallace and
366 Woodroffe, 2014). Earlier interglacials are MIS 13 (480-530 ka), MIS 15 (560-620 ka)
367 and MIS 17 (650-720 ka; Thompson et al., 2003; Andersen et al., 2008; Murray-
368 Wallace and Woodroffe, 2014). Fewer agreements exist in regards of the position of
369 the sea level during Pleistocene high-stands with respect to present (i.e eustatic sea-
370 level) and the estimates vary drastically. We compared the values from the last global
371 compilation of geomorphic Quaternary sea-level indicators (Murray-Wallace and
372 Woodroffe, 2014) with five eustatic sea-level curves (Table 1). The curves selected
373 (Waelbroeck et al., 2002; Bintanja and Van der Wal, 2008; Grant et al., 2014; Shakun
374 et al., 2015; Spratt and Lisiecki, 2016) encompass different reconstruction methods,
375 cover the time-range of interest (since MIS 11, 420 ka), and have their uncertainties
376 quantified. Murray-Wallace and Woodroffe (2014) analysing considerable amount of
377 literature, proposed that MIS 5e, MIS 7, MIS 9, and MIS 11 sea level high-stands
378 were, respectively, 6 ± 4 m higher, -8 ± 12 m lower, 3 ± 2 m higher, and 9.5 ± 3.5 m
379 higher than the modern sea level (Table 1). Waelbroeck et al. (2002) built a
380 composite relative sea-level curve over the last four climatic cycles from long benthic

381 isotopic records retrieved at one North Atlantic and one Equatorial Pacific site.
382 Bintanja and Van der Wal (2008) used both ice-sheet and ocean-temperature models
383 to extract 3 Ma mutually consistent records of surface air temperature, ice volume
384 and sea level from marine benthic oxygen isotopes. Grant et al. (2014) proposed a
385 chronology derived from a U/Th-dated speleothem $\delta^{18}\text{O}$ record, for a continuous,
386 high-resolution record of the Red Sea relative sea level over five complete glacial
387 cycles (~ 500 ka). Shakun et al. (2015) compiled 49 paired sea surface temperature-
388 planktonic $\delta^{18}\text{O}$ records and extracted the mean $\delta^{18}\text{O}$ of surface ocean seawater and
389 eustatic sea level over the past 800 kyr. Finally, Spratt and Lisiecki (2016) performed
390 principal component analysis on seven records from 0 to 430 ka and five records
391 from 0 to 798 ka (Spratt and Lisiecki, 2016).

392

393 Based on previous dating and our elevation measurements for the Pleistocene
394 shoreline angle, we derived uplift rates for North Cotentin. Eustasy-corrected uplift
395 rates are given by dividing the difference between the elevation of the shoreline
396 angle of dated marine terrace and the eustatic sea level at the time of its formation by
397 the age of the terrace (Lajoie, 1986). We also calculated the *apparent* uplift rates that
398 neglect any *a priori* eustatic correction (as in Pedoja et al., 2011; 2014; Yildirim et al.,
399 2013; Authemayou et al., 2017) (Table 1).

400

401 **3.6 Modeling the lower part of the sequence**

402

403 To propose ages for the undated low-standing marine terraces, T2 to T4, on the
404 Cape de la Hague (NW Cotentin), we used a synchronous correlation method as in
405 Roberts et al. (2013). We attempted to estimate uplift rates by searching for the best
406 match between the measured elevations of the successive shoreline angles with
407 those obtained by extrapolating uplift rates to the entire sequence of landforms. This
408 method initially assumes constant uplift rate, but with the option to test varying uplift
409 rates over time (Roberts et al., 2013). The Terrace Calculator is initially driven by age
410 controls. We extrapolated a fixed uplift rate of 0.01 mm/yr based on the Last
411 Interglacial Maximum (MIS 5e) dated terrace (122 ± 6 ka), present at elevations of \sim
412 5 ± 1 m. The output is the expected inner-edge elevations of the terraces allocated to
413 the high-stands from a chosen sea-level curve. These modeled shoreline angle
414 elevations are then matched against the measured one. Crucially, this method takes
415 into account re-occupation processes, i.e. old terraces can be erased by subsequent
416 high-stands, especially in a low uplifting area (e.g., Westaway, 1993; Roberts et al.,
417 2013). Herein, the Terrace Calculator relies on the sea-level curves from Siddall et
418 al., (2003) for 0-410 ka and Rohling et al. (2014) from 410-980 ka in the form of sea-
419 level relative to present-day and high-stand ages. To compare with estimates from
420 other sea-level curves, we used data from: Murray-Wallace and Woodroffe (2014)
421 from 0-400 ka, Grant et al. (2014) from 0-480 ka, Waelbroeck et al. (2002) from 0-

422 478 ka and Rohling et al. (2014) from 0 to 980 ka. Sea-level data from this latter
423 curve were also used to supplement the data within other models from their upper
424 age limits to 980 ka (see section 3.1).

425

426 **3.7 Database on Western European strandlines**

427 We expanded on Pedoja et al. (2011, 2014) databases on Cenozoic sequences of
428 strandlines that focused on MIS 5e and MIS 11 high-stands (supplementary data
429 Table 1). Here, we also provide information about: 1) sites where some MIS 7
430 landforms are present but landforms allocated to MIS 5e are lacking (supplementary
431 data Table 2); and 2) Neogene fossil shorelines (supplementary data Table 3).

432

433 **4 Coastal uplift of the Cotentin Peninsula**

434

435 **4.1 Distribution of the coastal sequences**

436

437 Our analysis reveals that the coastal sequences extend all over the Cotentin
438 Peninsula on a >200-km-long coastal stretch (Fig. 4-6). Depending on the occurrence
439 of the lower part of the sequence (i.e. marine terraces), we subdivided the peninsula
440 into three areas (Fig. 4A). North Cotentin is circumscribed by the English Channel

441 and the low-rising margin of the Seuil du Cotentin basin. South Cotentin is located
442 south of the Seuil du Cotentin basin. In between these two areas, in the Seuil du
443 Cotentin basin, no marine terraces are obvious in the landscape (Fig. 4A) but: **1)**
444 interglacial coastal deposits have been described using data from a borehole (see
445 section 4.4.3.); **2)** some rocky hills exhibit flat tops that we interpreted as shaped by
446 coastal erosion (emergence of rocky islets and platforms); and **3)** surface
447 classification model shows that the Seuil du Cotentin basin is a flat area, with a mean
448 elevation similar to that of the low lying terraces present in North and South Cotentin
449 (Fig. 3, 4A-C).

450

451 **4.1.1 The lower marine terraces: T1 to T4**

452

453 Along the shores of N Cotentin, the lower part of the sequence is laterally continuous
454 over ~110 km (Fig. 4D), from Saint-Vaast-la-Hougue in the Val de Saire area (east),
455 to Carteret (west). Such successive low-standing marine terraces are lacking where
456 elevated sea-cliffs are present, i.e. between the Nez de Jobourg and the north of
457 Anse de Vauville (Fig. 1C, 4D). The terraces and their deposits are frequently capped
458 by thick Pleistocene heads and loess (as in the Baie d'Ecalgrain, Fig. 4A) or are
459 heavily reworked by human activities (urban area of Cherbourg, Fig. 4A, 4E). The
460 width of the low part of the sequence (T1 to T4 marine terraces) ranges from a few
461 tens of metres (for instance at Port Racine) to a maximum of 6 km (Val de Saire).

462 The lower part of the sequence is the widest within the embayment (1 km at Urville
463 bay) and on Cape de la Hague (1.5 km). At the Cap de la Hague, from La Roche
464 (see Fig. 6A) to Port Racine, only the three lowest marine terraces are well
465 expressed in the landscape. T4 is locally present to the west (north of Auderville) as
466 a residual landform (paleo-peninsula or paleo-island?). Between Goury and Rocher
467 Gélétan (Fig. 5B), the lower strandlines have been eroded (i.e. formation of a low-
468 standing rasa). In the area, the 50 -to- 500 -m-wide T1 terrace has its distal edge at 5
469 \pm 1 m NGF (2 \pm 1 m above the modern shoreline angle; Table 1). Its shoreline angle
470 culminates at 7 \pm 1 m NGF (5 \pm 1 m above the modern shoreline angle). T2, as T1, is
471 50 to 500 m wide. Its distal edge is present at an elevation of 10 \pm 2 m NGF (7 \pm 2 m
472 above the modern shoreline angle) whereas its shoreline angle is present at 15 \pm 2 m
473 NGF (12 \pm 2 m above the modern shoreline angle). On the Cap de la Hague (Fig. 5A-
474 B), T1 and T2 strandlines conform to the modern shoreline; fossil beach deposits and
475 fossil sea stacks are associated to this terrace at Rocher Geletan and Hâvre de
476 Bombec sites (Fig. 5B), for example. On the Cap de la Hague, we observed deposits
477 associated to T1 marine terrace at 23 sites. These deposits are either 0.5 to 1.5 m -
478 thick layers of beach deposits comprised of a sandy matrix embedding sometimes
479 sorted centimetric to decimetric pebbles, suggesting only minor periglacial reworking,
480 and thinner deposits (0.5 m) of clay and silt with only a few metres of lateral extent.
481 These coastal deposits were reworked or capped by posterior periglacial processes
482 (solifluction) (Fig. 6B). T3 is 100 to 900 m wide and its distal edge is found at 17 \pm 2
483 m above the modern shoreline angle (20 \pm 2 m NGF). The shoreline angle of T3
484 culminates at 22 \pm 3 m above the modern shoreline angle (25 \pm 3 m NGF). Its

485 strandline does not conform to the modern one as it forms a fossil cape at the Rocher
486 Gélétan site (Fig. 5B). Finally, we infer the presence of T4 as a relict island or point
487 on the western side of the Cape de la Hague. The surface associated to T4 is
488 present at $\sim 33 \pm 3$ m.

489

490 **4.1.2 The upper rasas, R1 to R4**

491

492 All over the Cotentin Peninsula, we recognized four flat surfaces above the low-
493 standing marine terraces (Fig. 3 - 6). These surfaces are displayed over kilometres
494 and exhibit staircase morphology as they are separated by cliffs.

495

496 In N Cotentin, the sequence culminates at 185 ± 10 m (see rasa 4 on Fig. 4D). The
497 toe of the cliffs separating the staircase surfaces (i.e. rasas 1 to 3 of this study) are
498 respectively found at 167 ± 5 m, 138 ± 5 m and 86 ± 5 m (Fig. 4E). We discard the
499 hypothesis that such surfaces are the results of long-term periglacial weathering of
500 pre-existing continental surfaces. In our opinion, such weathering is unlikely to
501 generate regular staircase surfaces with similar elevations for each step (i.e. each
502 rasa) all over the peninsula. On La Hague Point (not to be confused with the Cap de
503 la Hague, the northern tip of La Hague Point), some of these cliffs were interpreted
504 as fault scarps associated with a NW - SE fault (Font et al., 2002; Lagarde et al.,

505 2003). However, morphologic and morphometric evidence suggests that these
506 landforms are fossil sea-cliffs not fault scarps. i) These cliffs, present on the
507 interfluves, are continuous in the landscape and on the DEM and not only observed
508 on La Hague Point (Fig. 4). Each individual cliff exhibits a circular or oblong pattern.
509 From map view, the outline shape of successive cliffs most generally conforms to the
510 lowest one and defines a concentric circular, or oblong, staircase coastal landscape
511 as observed for example on La Hague Point, to the south of Cherbourg, or to the
512 east of Barneville-Carteret (Fig. 4A). Such geometries (Fig. 4A) are difficult to relate
513 to the geometry of faults. ii) The inner-edge elevations of the planation surfaces
514 suggest that there are no elevation offsets at both sides of the Hague Point (Fig. 7A,
515 B) indicating that no tectonic movements took place along a purported fault running
516 along the elongated top of the Hague Point. In addition, we compared cliff heights
517 and their corresponding inner-edge elevations of each rasa level obtaining positive
518 correlations (Fig. 7C). Following the criteria proposed by Jara-Muñoz et al., (2017),
519 positive correlation suggests that these scarps were formed by the effect of coastal
520 erosion and uplift. In contrast, fault scarps usually characterized by negative or no
521 correlation. iii) Tectonic displacement due to this purported fault has been evoked to
522 explain the difference of elevations of the MIS 7 deposits at Ecalgrain and the MIS 5e
523 deposits on La Hague Point. Recent dating of the Ecalgrain deposits suggest a
524 reworking of MIS 7 deposits on the MIS 5e platform (i.e. re-occupation) (Cliquet et al.,
525 2009; Cliquet, 2015) which does not imply any activity of the purported fault.

526

527 In coastal areas, staircase flat surfaces with a circular or oblong pattern of the
528 successive cliffs are interpreted as the uplift and emergence of an island that further
529 coalesced with the nearby mainland (e.g., Szabo and Wedder, 1971; Lajoie et al.
530 1991; Pedoja et al., 2006 a,b; 2014; Authemayou et al., 2017). Hence, we interpret
531 the staircase planation surfaces of the Cotentin peninsula as rasas with their
532 associated shoreline angles.

533

534 In S Cotentin (Fig. 4F), the shoreline angles of the rasas R1 to R3 were found at
535 similar elevations within the error range of measurements to that of N Cotentin: $83 \pm$
536 5 m, 136 ± 5 , and 167 ± 5 m. Rasa 1 is best observed south of Avranches where it
537 constitutes wide surfaces ($> 3\text{km}$). Rasa 2 is the most extensive surface in the area
538 (width reaching 10 km) and Rasa 3 is morphologically better developed than in N
539 Cotentin. Rasa 4 caps the highest parts of the S Cotentin Peninsula with its distal
540 edge at 174 ± 5 m and its inner edge at 200 ± 5 m. The strandlines demonstrate a
541 convex segment of the coast (i.e. paleo-capes) locally interrupted by narrow
542 embayments, such as that observed east of Avranches.

543

544 **4.2 Paleogeographical evolution**

545

546 The distribution of the fossil strandlines in Cotentin provides strong evidence for the
547 emergence and coalescence of various rocky islands and islets, i.e. a rocky
548 archipelago, to form a bigger island that latter connected to the mainland through the
549 closure of the "Seuil du Cotentin" seaway. Such evolution began with the uplift of
550 rocky reefs and platforms to form the first islands of the archipelago. The size of such
551 islands typically ranges from few tens of metres to few kilometres with various
552 shapes; La Hague fossil island is oblong whereas La Boissais fossil island is more
553 circular. Such rocky platforms and low-lying islands compare with the modern
554 Chausey archipelago (Fig. 1B). Subsequently, the uplift concerns larger, flat rocky
555 islands bordered by shore platforms comparable to Alderney Island (Fig. 1B). The
556 islands further expand in size by the formation of successive rasas, and latterly,
557 marine terraces leading to larger and higher islands (as in Fig. 2) comparable to
558 Guernsey or Jersey where elevated marine terraces are also known (see Fig. 1B,
559 Renouf and James, 2011). Neighbouring rocky platforms result in the coalescence of
560 various elevated islands: six on N Cotentin and two overlooking the SW side of the
561 Seuil du Cotentin Basin (Fig. 4D). Through the closure of the Seuil du Cotentin
562 seaway, the N Cotentin main island (Rasa 1) was connected with the landmass, to
563 form the Cotentin Peninsula. This evolution is somehow schematic owing to the
564 interplay of tectonics, continental and marine erosion during earlier times, including
565 terrace re-occupation processes or, in theory, the emergence of terraces formed
566 during sea-level low-stands.

567

568 In summary, in N Cotentin the strandlines associated with the rasas define fossil
569 rocky islands and islets, while to the south of the Peninsula they define the
570 landmasses at the time of the emergence of the northern islands. We did not find
571 Cenozoic marine deposits associated with the rasas but they have been described
572 both to the north and south of the Peninsula (section 2.2).

573

574 **4.3 Upper Pleistocene (MIS 5e) uplift rates revisited**

575

576 We focused on dated terraces for which the elevations of the shoreline angles are
577 measured directly above their modern counterparts and calculated uplift rates for the
578 MIS 5e benchmark in N Cotentin. At various sites, its elevation above its modern
579 counterpart ($\sim 5 \pm 1$ m) implies an apparent uplift rate of 0.04 ± 0.01 mm/yr (Table 1).
580 The mean eustasy-corrected uplift rates have large margins of error (Table 1).
581 Depending of the sea-level data used, their mean values can be either: i) slightly
582 negative: -0.01 ± 0.04 mm/yr (data from Murray-Wallace and Woodroffe (2014)), ii)
583 neutral: 0.00 ± 0.11 mm/yr (data from Waelbroeck et al. (2002) or 0.00 ± 0.13 mm/yr
584 (data from Spratt and Lisiecky (2016)) or iii) positive: 0.04 ± 0.08 mm/yr, 0.13 ± 0.12
585 mm/yr and 0.01 ± 0.12 mm/yr (data from Bintanja and Van Der Wal (2008), Shakun
586 et al. (2015) and Rohling et al. (2014) respectively). As previously noted for the
587 sequence of NE Cotentin, subsidence is unlikely since the coastal staircase
588 morphology is clearly associated with uplift (Coutard et al., 2006). For T1 and T2, an

589 error of ± 12 m for the predicted elevations for each high-stand is directly taken from
590 Siddall et al. (2003). T3 and T4 have a higher error of 35 m as per the discussion in
591 Rohling et al. (2014). As some of these errors are larger than the elevations of the
592 terraces used, we applied statistical testing to interpret the relationship between a set
593 of predicted elevations versus measured elevations (see below).

594

595 Whichever correction is applied, Upper Pleistocene coastal uplift rates are low to very
596 low (< 0.2 or <0.1 mm/yr, respectively, as in Pedoja et al. (2011)) as observed
597 elsewhere along the Western European coasts (section 5.3) or along other passive
598 margins (Pedoja et al., 2014).

599

600 **4.4 Possible timings for the emergence of the Peninsula**

601

602 To obtain a chronological framework for the undated landforms, we postulated steady
603 uplift rates (Lajoie, 1986), although this is unlikely at the timescales considered. We
604 extrapolated three possible rates derived from: (i) the elevation of the dated MIS 5e
605 terrace; (ii) the elevations of T2 to T4 allocated to MIS 7, 9 and MIS 11 (short lasting
606 hypothesis, as in Coutard et al., 2006) (Fig. 8A) and; (iii) modelling of the lower
607 sequence (long lasting hypothesis, Fig. 8B, 9). These are further explored below.

608

609

4.4.1 Short-lasting hypothesis

610

611 In N Cotentin, the "standard method" (Table 2) which sequentially correlates each
612 subsequently higher terrace to the next older high-stand, consists of the allocation of
613 T2, T3 and T4 to MIS 7, MIS 9 and MIS 11, respectively (as in Coutard et al., 2006).
614 It results in homogeneous apparent uplift rates ($\sim 0.06 \pm 0.03$ mm/yr; Table 2). When
615 corrected for eustasy, variations in the uplift rates are clear and show an increase of
616 uplift during the penultimate interglacial whatever the correction applied (Table 2, Fig.
617 8A). Consequently, we extrapolated a mean MIS 5e apparent uplift rate of $0.04 \pm$
618 0.01 mm/yr, and a mean "high" Middle Pleistocene eustasy-corrected of 0.09 ± 0.03
619 mm/yr (Table 3).

620

621 On N Cotentin, rasa 4 caps the paleo-islands of La Hague and La Boissais at
622 elevations of 185 ± 10 m (Fig. 8A). Both islands would have emerged at 5 ± 1.5 Ma
623 (apparent) or 2.9 ± 0.9 Ma (eustasy-corrected) (see Table 3 for the possible age of
624 formation of the other rasas). In summary, the short-lasting hypothesis suggests a
625 Pliocene onset of the sequences preserved on the peninsula.

626

627

4.4.2 Long-lasting hypothesis

628

629 Synchronous correlation modelling (as in Roberts et al., 2013) suggests that a
630 constant uplift rate of 0.01 mm/yr (Table 4) would be responsible for the formation
631 and preservation of the four low terraces (T1-T4) on N Cotentin. The shoreline angle
632 of the last interglacial maximum T1 marine terrace is found at $\sim 5 \pm 1$ m above its
633 modern counterpart and has a predicted elevation of 6 m. Modelling suggests that T2
634 (at 12 m) would be correlated with the 340 ka high-stand (MIS 9c, predicted to be at 8
635 m). T3 (at 22 m) would be allocated to either the MIS 13 (525 ka) or MIS 15 (620 ka)
636 high-stand predicted to be both at 26 m (Table 4, Fig. 8B and 9). Finally, T4 (at 33 m)
637 would be assigned to the 980 ka high-stand predicted to be at 35 m. The modelling
638 suggests reoccupation processes for the high-stands between MIS 5e and MIS 9c,
639 as well as for those between MIS 9c and MIS 15 (numbers in grey scale, Table 4).
640 Such processes, symptomatic of low uplift, have also been observed at Menez
641 Dregan (W Brittany, Table 1 supplementary data) where both MIS 5e and MIS 11
642 coastal deposits are present on the same terrace. In our analysis, T2 was allocated
643 to the MIS 11 high-stand using eustasy-correction from either Waelbroeck et al.
644 (2002) (predicted to be at 10 m) or Murray-Wallace and Woodroffe et al. (2014)
645 (predicted to be at 14 m). As sea-level data from these curves does not extend
646 beyond 478 ka, the allocations of T3 and T4 did not alter when they were tested. We
647 assessed the relationship between the predicted and measured elevations using a
648 non-parametric method – Pearson's correlation coefficient with an output of $r = 0.99$,
649 approaching the ideal value of 1 (Fig. 9A). This indicates a robust correlation
650 between multiple strandline elevations and multiple sea-level high-stands, which
651 would imply that uplift rates have not varied over the last 0.5 Ma.

652 We compared the RMS deviation of all uplift rates scenarios from 0 to 0.11 in
653 intervals of 0.005 in order to assess the accuracy of the constant uplift rate we
654 obtained from the dated shoreline (Fig. 9B). An uplift rate of 0.01 mm/yr constant
655 over ~ 1 Ma provides the best fit uplift rate to model the coastal sequences of the
656 Cotentin Peninsula (Fig. 9B). Extrapolating such a rate yields that Rasa 4 would have
657 emerged at 18.5 ± 1 Ma, Rasa 3 at 16.5 ± 0.5 Ma, Rasa 2 at 13.8 ± 0.5 Ma and Rasa
658 1 at 8.6 ± 0.5 Ma (Table 3, Fig. 8C). Assigned rasa ages are in good agreement with
659 Neogene-aged high-stands (Miller et al., 2005). R4, R3 and R2 would record the
660 following highstands; ~ 17.5-18.5 Ma (early Miocene), 14.5 Ma (middle Miocene),
661 13.5 - 12 ka (late Miocene). Finally, R1 would be the morphological expression of the
662 intensification of the sea-level oscillations during the late Miocene-Pliocene and early
663 Pleistocene.

664 In short, the long-lasting hypothesis emphasizes an early Miocene onset of the
665 coastal sequence preserved on the Cotentin Peninsula.

666

667 **4.4.3 Age of the onset of the coastal sequences?**

668

669 Both uplift hypothesis (i.e. short versus long-lasting) fit with previous descriptions of
670 Miocene and Pliocene coastal deposits overlying the rasas (see section 2.1). The
671 combination of hypotheses results in a very large age range. Rasa 4 would have

672 emerged between 1.5 and 19.5 Ma considering all the errors within the extrapolation
673 (Table 3).

674

675 The timing of the closure of the seaway that once formed the Seuil du Cotentin area
676 provides crucial data to assess the age of the coastal sequences located in its
677 vicinity. Based on boreholes and sparse outcrops, the thickness of the marine to
678 fluvial sediments deposited in the Seuil du Cotentin basin is estimated to be > 150 m.
679 The sediments consist of clastic deposits with conglomerates and peat at the top of
680 the formation. The depositional environments of the succession change from marine
681 to fluvial and represent two transgression–regression cycles (Dugué, 2003). In many
682 studies (Clet-Pellerin et al., 1997; Garcin et al, 1997; Dugué et al., 2007, 2009) this
683 sequence is interpreted as being deposited during Late Pliocene to Early
684 Pleistocene. The first transgression identified is referred to as the "Brunssumian–
685 Reuverian", which approximates to the whole Pliocene and the associated deposits
686 are now found offshore in the English Channel (Dugué, 2003). The second
687 transgression is proposed to be Lower Pleistocene (Tiglian, 2.4-1.8 Ma) associated
688 with the Sable de Saint Vigor Formation. Clet-Pellerin et al. (1997) proposed an age
689 of 1.45 - 1.2 Ma (MIS 34 - 36) in comparison with other European sites. However, the
690 exact correlations between these local stages and the international chronological
691 stages remain unknown. More recently, van Vliet-Lanoë et al. (2002) proposed for
692 the Sable de Saint Vigor, through direct Sr dating, a Zanclean (Pliocene) age for the
693 formation.

694

695 At this stage, more dating is needed to better constraint the timing of the onset of the
696 coastal sequences preserved on the Cotentin Peninsula.

697

698 **5 Late Cenozoic uplifting coastal sequences of Western Europe**

699

700 Early descriptions of marine terraces and raised beaches arise from the English
701 Channel shores mostly because low-standing coastal deposits and overlying
702 continental cover both contain flints and extinct mammal bones (e.g Lyell, 1830;
703 Moore, 1842; Chambers, 1848; Prestwich, 1862-1863; Breuil et al., 1942). Early
704 syntheses on sequences of strandlines dealt with Western Europe and more
705 specifically with sites in western France and southern England (e.g., Barrell, 1915;
706 Depéret, 1918-1922; Daly, 1925; Wythe-Cooke, 1930; Bull, 1941; Baden-Powell,
707 1954; Guilcher, 1969). This area is rather neglected in recent global synthesis on sea
708 - level changes (e.g. Pedoja et al., 2014; Murray-Wallace and Woodroffe, 2014).

709

710 Out of 180 references (supplementary data Tables 1, 2, 3), we evidenced: 1) 169
711 sequences embedding the MIS 5e benchmark (99 sites in Pedoja et al. 2014), 2) two
712 sequences including coastal landforms and deposits correlated to MIS 7 but no
713 strandline correlated to the last interglacial maximum (MIS 5e), 3) 14 sequences

714 including the MIS 11 shoreline; and 4) 21 sequences including some Neogene
715 strandlines.

716

717 At any coastal site, current elevations of the Holocene and Pleistocene terraces
718 depend on the combination of glacio-isostatic adjustment (GIA), tectonics and other
719 local processes (Shennan and Horton, 2002; Milne et al., 2005). In France, Spain
720 and Portugal, the lack of accurate Holocene sea-level index points precluded the
721 establishment of Holocene sea-level curves but recent advances have been made
722 from the analysis of submerged deposits in estuaries (e.g., Leorri et al., 2012).
723 Lambeck, (1991; 1996) and Shennan and Horton, (2002) constrained Late
724 Pleistocene and Holocene relative sea level changes in the British Isles and provided
725 estimates of current land-level changes (negative of relative sea-level change).
726 Maximum relative land uplift occurs in central and western Scotland, at $\sim 1.6 \text{ mm yr}^{-1}$,
727 and maximum subsidence is in southwest England, at $\sim 1.6 \text{ mm yr}^{-1}$. As our aim is to
728 evidence the Neogene - Quaternary tectonic uplift of western European coasts, we
729 do not consider, in our interpretation, sequences located in areas where fast GIA
730 dominates the signal, as evidenced by Lambeck, (1987; 1991) and Shennan and
731 Horton, (2002; see dotted line Fig.10A). In area where the last GIA is inducing
732 subsidence (i.e. Southern England), tectonic uplift is lowered. Of course such
733 quantifications only concern the period following the last glacial (MIS 2). In the case
734 of MIS 5e marine terraces, two joint corrections could be applied because one should
735 ideally compare the shape of the Earth deprived of GIA, therefore compare a GIA-

736 relaxed MIS 5e (i.e. without any GIA from the previous deglaciation stage MIS 6),
737 with a present-day GIA-relaxed Earth. This lack of knowledge on Middle Pleistocene
738 GIA prevents correcting MIS5e uplift rates. Consequently for the British Isles, we
739 discarded 64 sites (underlined in grey on supplementary Table 1) where older, Middle
740 Pleistocene, highstands (MIS 7, 9, MIS 11) are absent and where MIS5e is not
741 embedded within a longer lasting sequence.

742

743 At many sites along the coasts of Spain, Portugal and France, sequences are
744 morphologically similar to that of Cotentin: low-standing, rather well-individualized
745 fossil rocky strandlines, overlooked by older, wider rasas. In NW Portugal (Minho
746 area), five marine terraces reach 65 ± 5 m in elevation and are overlooked by a rasa
747 culminating at 100 m (e.g., Texier and Meireles, 1987). In France, within the Brest
748 embayment (Feunteunaon site Table 1 Supplementary data), a sequence of six
749 terraces and rasas reach 135 m in elevation (Guilcher, 1974; Hallégouët, 1976).
750 Fossil landforms frequently consist in rocky shore platforms with associated deposits
751 (e.g., rasa and marine terraces), sea caves with coastal deposits (e.g. Sutcliffe et al.,
752 1987), or fossil depositional landforms such as the Plovan beach ridge (Guilcher and
753 Hallégouët, 1981). Most sequences are strongly affected by continental erosion.
754 Remnants of marine terraces and rasas, preserved on the interfluves, are often
755 capped by continental deposits: heads and loess to the north (e.g., Regnault et al.,
756 2003), aeolian and alluvial deposits to the south (e.g., Teixeira, 1944). In Spain and
757 Portugal, rasas are obvious in the landscape and frequently include coastal deposits.

758 In France, rasas are more dissected and show fewer deposits that are often azoic.
759 Rasas, whether sedimentary (e.g., Portugal, see Cunha et al., 2015a, 2015b) or
760 erosive, are more intensely dissected by fluvial erosion than younger marine terraces
761 (for instance in the Pays de Leon, Brittany, e.g., Hallégouët, 1976). Within estuaries,
762 sequences are composite, made of both marine and fluvial terraces, as observed in
763 Portugal (e.g., Ramos et al., 2012), Spain (Moreno and Mediato, 2009), France (e.g.,
764 Hallégouët, 1976) or England (Westaway et al., 2009).

765

766 Dating indicates that the lowest standing coastal landforms were formed during MIS
767 5e high-stand (Table 1 supplementary data) for which we compiled its elevation at
768 169 sites. Two studies propose a different morpho-stratigraphy for some marine
769 terraces deposits in Portugal and Spain. On the basis of ^{14}C and OSL dating,
770 Benedetti et al. (2009) correlated some of the low-standing terraces in Estremadura
771 (Portugal) to MIS 3 and 4. Through ^{14}C dating, González-Acebrón et al., (2016) also
772 correlated low-standing terraces to MIS 3 in southern SE Spain, next to Cadiz. We
773 discard these results since they are not benchmarked on the same MIS 5e, MIS 11 or
774 older sea level high-stands that we consider herein.

775

776 At two sites, strandlines older than MIS 5e are present whereas MIS 5e is lacking
777 (Fig. 10B and Table 2 supplementary data). At Sangatte (N France), long-recognized
778 coastal deposits and morphologies (e.g., Prestwich, 1851, 1865; Baudet, 1959), were

779 dated by OSL and correlated to MIS 7 (Balescu et al., 1992), but the sedimentary
780 coastal sequence could also include MIS 9 deposits (Sommé et al., 1989; 1999). At
781 Easington (Eastern England), in an area affected by post glacial rebound (uplift)
782 raised beach deposits associated to a fossil strandline were dated by OSL and
783 amino-acid racemization and correlated to MIS 7 high-stand (Davies et al., 2009).
784 Older dated geomorphic markers consist in MIS 11 strandlines, described at 14 sites
785 (Table 1 supplementary data). Finally, rasas overlook individualized strandlines at 21
786 sites (Fig. 10C, Table 3 supplementary data). At a limited number of sites in SW
787 Europe, marine deposits or marine surfaces associated with the rasas have been
788 dated (Fig. 10C, Table 3 supplementary data). The dating is absolute (^{10}Be ; Sr) as for
789 the Rasa of Cerro da Boa Viagem (Portugal) or the 60 -m-high rasa of Cantabria
790 (Spain) or relative (biostratigraphy, geometry of discordance, etc.) (Table 3
791 supplementary data). A Miocene (Aquitano-Langhense) onset is proposed for the
792 sequence of central and western Asturias (Spain) where the highest rasa has an
793 elevation of 264 m and 180 m respectively (Table 3 supplementary data). In Portugal,
794 the onset of the sequences is proposed to be Pliocene (Table 3 supplementary data,
795 sites Serra da boa Viagem, Lavos-Alqueidao, Maiorca - Vila Verde or Cabo Espichel
796 for example). Comparison with similar sites around the world shows that Pliocene or
797 Miocene ages for the initiation of some coastal sequences are still discussed, for
798 example in Casablanca (Morocco, Raynal et al., 1999).

799

800 Within the studies compiled, elevation measurements are generally provided above
801 the Principal Datum of the considered country (e.g., NGF for France, O.D. for
802 England; see section 2.2). Yet, studies where elevations measurements are
803 discussed are scarce (e.g., Arkell, 1943; Alonso and Pages, 2000; Coutard et al.,
804 2006; Figueiredo et al., 2013).

805

806 At various sites, the mean elevation of the shoreline of the last interglacial maximum
807 stands within estimates for the eustatic range of MIS 5e sea level with respect to
808 present-day (Siddall et al., 2006; Kopp et al., 2009; Rohling et al., 2009). However, in
809 Western Europe as elsewhere (Pedoja et al., 2014; Authemayou et al., 2017), MIS 5e
810 marker is always embedded within a staircase coastal sequence, a morphology that
811 cannot be explained in the absence of regional uplift.

812

813 Excluding areas affected by fast GIA, in our database, the elevation of MIS 5e
814 benchmark ranges from -2 ± 1 m (site Le Havre, France, Breton et al., 1991) to 19.5
815 ± 1 m at Tarifa (Atlantic Southern Spain, Zazo et al., 1999) with a mean of 6.2 m \pm
816 1.6 m (Table 3 supplementary data). Elevations of Middle Pleistocene MIS 11
817 landforms range from 8 ± 3 m to 33 ± 4 (mean 20 ± 2.5 m). Consequently, upper
818 Pleistocene (MIS 5e) apparent uplift rates range from -0.016 ± 0.008 mm/yr to $0.16 \pm$
819 0.01 mm/yr with a mean of 0.05 ± 0.01 mm/yr (Fig. 10A). Apparent Middle
820 Pleistocene uplift rates range from 0.02 ± 0.01 to 0.08 ± 0.02 mm/yr (mean $0.05 \pm$

821 0.01 mm/yr) (Fig. 10B). The modern elevation of rasas indicates long-term tectonic
822 uplift of Western Europe (Spain, Portugal, France, and possibly UK and Ireland) as
823 such landforms cannot be explained by the sole effect of eustasy. Mean apparent
824 long-term uplift rates are ~ 0.01 mm/yr, (Table 3 supplementary data, Fig. 10C) and
825 are consistent with previous estimates of ~ 90 m of Pleistocene uplift from fluvial
826 incision measurement in the coastal area (ca. 0.03 mm/yr; Bonnet et al., 2000; Brault
827 et al., 2004).

828

829 Pleistocene and Neogene coastal uplift rates of Atlantic Europe are low to very low (~
830 0.01 to 0.2 mm/yr, as in Pedoja et al., 2011) and rather uniform over the studied
831 zone, though with local exceptions that we cannot address without further dating
832 (e.g., MIS 7 at Sangatte, see Table 1 supplementary data). At first glance, the
833 convergence between Eurasia and Africa induces more intense deformation to the
834 south in southern Spain and Portugal (e.g. see Ingrina or Conil-Trafalgar data, Table
835 1 supplementary data). But, before any detailed interpretation, these data need to be
836 refined especially for rasa sites where deposits are present.

837

838 Our findings are in line with earlier studies that suggest that a Neogene tectonic
839 event affected most continental margins of Atlantic Europe, and reached far into the
840 European craton (e.g., Japsen and Chalmers, 2000). Similar vertical movements are
841 reported for other continental margins (e.g., Japsen et al., 2006; Bonow et al., 2009),

842 and are not unique to the Late Cenozoic (Peulvast et al., 2008; Bertotti and Gouiza,
843 2012). These facts taken together call for a common underlying process. These
844 anomalous vertical motions ought to have a large-scale tectonic origin, regardless of
845 the subjacent proposed mechanism, which remains a matter of debate. Possible
846 mechanisms are igneous underplating (Brodie and White, 1994), asthenospheric
847 upwelling, isostatic readjustments due to glacial erosion and regional compression of
848 the lithosphere (e.g. Japsen and Chalmers, 2000; Yamato et al., 2013). We favour
849 the latter for it fits with the large-scale distribution of the coastal uplift evidenced from
850 southern Spain to Northern Ireland (Fig. 1A, 10). In an attempt to reframe the Atlantic
851 coastal uplift of Europe in its entirety, we emphasize that, alike mountain belts
852 worldwide, uplifting coasts of western Europe are symptomatic of the generalized
853 lithospheric compression that increased during the Cenozoic (Yamato et al., 2013).
854 Collisions at far-field plate margins overall increase compression in lithospheric
855 plates; tectonic inversion, and uplifting continental margins reveal this augmenting
856 stress regime worldwide (Pedoja et al., 2011; Japsen et al., 2012; Yamato et al.,
857 2013). Similar regional illustrations are found in Greenland (e.g., Døssing et al.,
858 2016), southern Africa (Green et al., 2016), or Brazil (Japsen et al., 2012). Ultimately,
859 this compression is induced by mantle convection underneath tectonic plates
860 (Yamato et al., 2013; Husson et al., 2015; Walker et al., 2016) and is most probably
861 expressed through the widespread Neogene and Quaternary sequence of coastal
862 landforms (marine terrace rasas) found along the shores of Western Europe.

863

864 **6 Conclusion**

865

866 On the Cotentin Peninsula, the typical coastal sequence culminates at ~200 m and
867 includes up to four low-rising, clearly distinguished marine terraces overlooked by up
868 to four rasas. Based on previous dating of the last interglacial maximum (MIS 5e)
869 marine terrace in N Cotentin, as well as on modelling, we derived: 1) a mean Upper
870 Pleistocene (MIS 5e) apparent uplift rate of 0.04 ± 0.01 mm/yr; 2) a mean "high"
871 Middle Pleistocene eustasy-corrected of 0.09 ± 0.03 mm/yr and 3) a low constant
872 uplift rate of 0.01 mm/yr using a synchronous correlation approach. Extrapolation of
873 these rates reveals that the onset of the sequence of N Cotentin Peninsula started
874 between ~ 3 Ma and ~ 15 Ma ago. The palaogeographic evolution of the Cotentin
875 Peninsula (Normandy, France) corresponds to the emergence of rocky islands and
876 islets that gradually merged together, and thereafter to the continent, ultimately
877 forming a peninsula. Furthermore, through compilation of former data, we highlight
878 that such morphostratigraphy - Pleistocene terraces overlooked by widespread Mio-
879 Pliocene rasas - is representative of Western Europe (except the British Isles) and, to
880 a larger extent, is related to the generalized Cenozoic compression that accompanies
881 the convergence between Africa and Eurasia.

882

883 **Acknowledgments:** We thank the ANR GiSeLE as well as the INSU programme
884 Sulamer Hople for funding. This research is in memoriam of Jean Pierre Lautridou
885 who has shown the coastal sequences of North Cotentin to many of us.

886

887 **Figure Captions**

888

889 **Figure 1:** Index map **A)** Location of the Cotentin Peninsula in W Europe **B)** Coastal
890 sequences in Normandy and Northern Brittany. Stars represent sites where a
891 sequence of coastal landforms (marine terraces, raised beaches) includes the MIS
892 5e benchmark (data from Pedoja et al., 2011, 2014, see Table 1 supplementary
893 data). **C)** Location of Plio-Pleistocene basins on the Cotentin Peninsula. Extents of
894 Plio-Pleistocene basins from Dugué (2003). **1** Larmor-Pleubian, **2** Brehat, **3** Binic, **4**
895 Cesson, **5** Port Morvan, **6** Dahouet, **7** Piegu, **8** NE Saint Malo, **9** Hacqueville, **10**
896 Hauteville - Annoville, **11** Chausey, **12** Jersey, **13** and **14** Guernsey SE and W. **15** le
897 Rozel, **16** Alderney, **17** St Martin Jerd'heux, **18** Val de Saire, **19** Grandcamp Maisy,
898 **20** St Côme - Asnelle - Meuvaine, **21** Graye, **22** le Havre. **Is** Island. **Ar** Archipelago.
899 **LM** La Mondrée submerged terrace. **SV** Saint Sauveur le Vicomte. **SM** Sainteny
900 Marchésieux. Stars : coastal sequences including the MIS 5e landforms (Pedoja et
901 al., 2011; 2014). Line : uplifted coastal stretch (Pedoja et al., 2014; this study).

902

903 **Figure 2 :** Idealized staircase coastal landscape. **A)** Sequence of marine terraces
904 and rasas. **B)** Detail of a single marine terrace. **C)** Elevation transects.

905

906 **Figure 3 :** Extent of the high-resolution topography and results of the regional
907 morphometric analysis. **A)** Shaded topography and high-roughness patches
908 identified using the Surface Classification Model (SCM). **B-C)** results of surface
909 classification model SCM **D-E)** Example of SCM classification and mapping of marine
910 terrace surfaces. **E-F)** Histograms of slope and roughness used to calibrate the SCM,
911 selected ranges include 90% of the data.

912

913 **Figure 4:** The coastal sequences of the Cotentin Peninsula. **A)** Surface classification
914 model displaying flat surfaces interpreted as sequences of marine terraces and
915 rasas. **B - C)** Histogram of elevation v/s surface of SCM patches of N and S Cotentin.
916 Levels are defined using elevation ranges, the width of each band represent the
917 position of the outer and inner edge of marine terraces and rasas. **D)** Schematic
918 mapping of North Cotentin marine terrace and rasas. **E) - F)** Swaths profiles across
919 the Cotentin Peninsula, north and south, respectively.

920

921 **Figure 5:** Coastal sequence at Point and Cape de La Hague. **A)** General mapping **B)**

922 Detailed mapping **C)** GPS Profile

923

924 **Figure 6:** Interpreted pictures of the sequence in N. Cotentin **A)** Low-standing T1

925 terrace at Goury **B)** Rasa and covered sequence of Ecalgrain Embayment **C)** Low-

926 standing terrace at Anse de Vauville.

927

928 **Figure 7:** Morphometry of the rasa surfaces at La Hague Point. **A)** Surface

929 classification model and swath profiles (black rectangles) used to map inner edges

930 (black dots). **B)** Box plot of inner edge elevations for each rasa at both sides of La

931 Hague Point. Dashed lines indicate the mean elevation. Notice that the difference

932 between inner edges at both sides of the ridge is less than 2 m. **C)** Scatter plots of

933 cliff height versus inner edge elevations of each rasa. Red line is a lineal regression

934 and associated correlation coefficient (R^2), notice positive slope suggesting that

935 these cliffs were formed by sea erosion (see text for further details).

936

937 **Figure 8:** Hypothesis on the timing of formation of the sequence from N Cotentin **A)**

938 The sequence with dated terrace and elevations of the strandlines **B)** the short-

939 lasting hypothesis : Pliocene onset of the Cotentin coastal sequences **C)** the long-

940 lasting hypothesis: Miocene onset of the Cotentin coastal sequences.

941

942 **Figure 9:** Synchronous correlation method applied to the four (T1 to T4) low-standing
943 terraces in Cotentin. Methods as in Roberts et al., 2013. **A)** Predicted versus
944 measured elevations of the shoreline angle of the low-standing marine terraces of N
945 Cotentin **B)** Uplift rates and RMS deviation

946

947 **Figure 10:** Coastal uplift of Western Europe **A)** MIS 5e. The dotted line represent for
948 the British Isles, the frontier between uplifting coasts (to the north) and subsiding
949 coasts (to the south), for the period of time 0-6 ka as in Lambeck, (1991; 1996) and
950 Shennan and Horton, (2002). see text for more details **B)** MIS 11 and MIS 7 isolated
951 **C)** Old shorelines

952

953 **Table 1:** Mean Upper Pleistocene Coastal Uplift rates of N Cotentin

954

955 **Table 2:** Hypothesis on middle Pleistocene apparent and eustasy-corrected uplift
956 rates of North Cotentin

957

958 **Table 3:** Hypothesis on the age of the upper rasas extrapolating various uplift rates

959

960 **Table 4:** Result of the synchronous method modelling, elevations in red indicate that
961 younger sea-level high-stands would destroy the older high-stand shorelines or, in
962 some cases, suggest that shorelines and their terraces may be caused by more than
963 one sea-level high-stand.

964

965 **References cited**

966

967 Allard, M. and G. Tremblay (1981). "Observations sur le Quaternaire de l'extrême-orientale de la péninsule de Gaspé, Québec." Géographie physique et Quaternaire **35**(1): 105-125.

970

971 Alonso, A. and J. L. Pagés (2000). "El registro sedimentario del final del cuaternario en el litoral noroeste de la península Iberica. Margenes Cantábrico y Atlántico." Revista de la Sociedad Geológica de España **13**(1): 17-29.

974

975 Alvarez-Marrón, J., R. Hetzel, S. Niedermann, R. Menéndez and J. Marquínez (2008). "Origin, structure and exposure history of a wave-cut platform more than 1 Ma in age at the coast of northern Spain: A multiple cosmogenic nuclide approach." Geomorphology **93**(3-4): 316-334.

979

980 Andersen, M. B., C. H. Stirling, E.-K. Potter, A. N. Halliday, S. G. Blake, M. T.
981 McCulloch, B. F. Ayling and M. O'Leary (2008). "High-precision U-series
982 measurements of more than 500,000 year old fossil corals." Earth and
983 Planetary Science Letters **265**(1-2): 229-245.

984

985 Antoine, P., J.-P. Coutard, P. Gibbard, B. Hallegouet, J.-P. Lautridou and J.-C. Ozouf
986 (2003). "The Pleistocene rivers of the English Channel region." Journal of
987 Quaternary Science **18**(3-4): 227-243.

988

989 Antoine, P., J. P. Lautridou, J. Sommé, P. Auguste, J. P. Auffret, S. Baize, M. Clet-
990 Pellerin, J.-P. Coutard, Y. Dewolf, O. Dugué, F. Joly, B. Laignel, M. Laurent,
991 M. Lavollé, P. Munaut, P. Lebret, F. Lécolle, D. Lefebvre, N. Limondin-
992 Lozouet, A.-V. Munaut, J.-C. Ozouf, F. Quesnel and D. Rousseau (1998). "Les
993 formations quaternaires de la France du Nord-Ouest : Limites et corrélations
994 [The quaternary formations of North-West France :" Quaternaire **9**(3): 227-
995 241.

996

997 Arkell, W. J. (1943). "The Pleistocene rocks at trebetherick point, north Cornwall:
998 their interpretation and correlation." Proceedings of the Geologist's Association

999 LIV(part 4): 141-170.

1000

1001 Auffret, J.-P., D. Alduc, C. Larsonneur and A. J. Smith (1980). "Cartographie du
1002 réseau des paléovallées et de l'épaisseur des formations superficielles
1003 meubles de la Manche orientale." Annales de l'Institut Océanographique,
1004 Paris **58**(8): 21-35.

1005

1006 Authemayou, C., K. Pedoja, A. Heddar, S. Molliex, A. Boudiaf, B. Ghaleb, B. Vliet
1007 Lanoe, B. Delcaillau, H. Djellit, K. Yelles and M. Nexer (2017). "Coastal uplift
1008 west of Algiers (Algeria): pre- and post-Messinian sequences of marine
1009 terraces and rasas and their associated drainage pattern." International
1010 Journal of Earth Sciences: 1-23.

1011

1012 Baden-Powell, D. F. W. (1955). "The correlation of the Pliocene and Pleistocene
1013 marine beds of Britain and the Mediterranean." Proceedings of the Geologists'
1014 Association **66**(part 4): 271-292.

1015

1016 Baize, S. (1998). Tectonique, eustatisme et climat dans un systeme
1017 geomorphologique cotier. Le nord-ouest de la france au plio-pleistocene :
1018 exemple du cotentin (normandie). Géologie. Caen, University of Caen: 333 p.

1019

1020 Balescu, S., S. C. Packman, A. G. Wintle and R. Grün (1992). "Thermoluminescence
1021 dating of the middle Pleistocene raised beach of Sangatte (Northern France)."
1022 Quaternary Research **37**(3): 390-396.

1023

1024 Ballèvre, M., V. Bosse, C. Ducassou and P. Pitra (2009). "Palaeozoic history of the
1025 Armorican Massif: Models for the tectonic evolution of the suture zones."
1026 Comptes Rendus Geoscience **341**(2-3): 174-201.

1027

1028 Barrell, J. (1915). "Factors in movements of the strand line and theirs results in the
1029 Pleistocene and Post-Pleistocene." American Journal of Science Fourth
1030 Series XL(235): 1-22.

1031

1032 Bates, M. R., D. H. Keen and J. P. Lautridou (2003). "Pleistocene marine and
1033 periglacial deposits of the English Channel." Journal of Quaternary Science
1034 **18**(3-4): 319-337.

1035 Battistini, R. and J. P. Bergoeing (1982). "Un exemple de côte à structure faillée
1036 quadrillée et néotectonique active : la côte pacifique du Costa Rica (The
1037 pacific coast of Costa Rica)." Bulletin de l'Association de géographes français
1038 **487-488**: 199-205.

1039

1040 Baudet, J.-L. (1959). "Les industries des plages suspendues (de 5m) du Nord de la
1041 France." Bulletin et Mémoires de la Société d'anthropologie de Paris Xe série.
1042 **Tome 10** (Fascicule 4): 285-301.

1043

1044 Bauer, H., P. Bessin, P. Saint-Marc, J.-J. Châteauneuf, C. Bourdillon, R. Wyns and F.
1045 o. Guillocheau (2016). "The Cenozoic history of the Armorican Massif: New
1046 insights from the deep CDB1 borehole (Rennes Basin, France)." Comptes
1047 Rendus Geoscience **348**(5): 387-397.

1048

1049 Benabdellouahed, M., O. Dugué, B. Tessier, I. Thinon and P. Guennoc (2013).
1050 "Evolution pléistocène de la Seine fluviatile préservée en Baie de Seine."
1051 Bulletin de l'Association Française pour l'Etude du Quaternaire **24**(3): 267-277.

1052

1053 Benedetti, M. M., J. A. Haws, C. L. Funk, J. M. Daniels, P. A. Hesp, N. F. Bicho, T. A.
1054 Minckley, B. B. Ellwood and S. L. Forman (2009). "Late Pleistocene raised
1055 beaches of coastal Estremadura, central Portugal." Quaternary Science
1056 Reviews **28**(27-28): 3428-3447.

1057

- 1058 Bertotti, G. and M. Gouiza (2012). "Post-rift vertical movements and horizontal
1059 deformations in the eastern margin of the Central Atlantic: Middle Jurassic to
1060 Early Cretaceous evolution of Morocco." International Journal of Earth
1061 Sciences **101**(8): 2151-2165.
- 1062
- 1063 Bessin, P., F. Guillocheau, C. Robin, J.-M. Schroëtter and H. Bauer (2015).
1064 "Planation surfaces of the Armorican Massif (western France): Denudation
1065 chronology of a Mesozoic land surface twice exhumed in response to relative
1066 crustal movements between Iberia and Eurasia." Geomorphology **233**: 75-91.
- 1067
- 1068 Bigot, A. (1897). "Sur les dépôts pléistocènes et actuels du littoral de la Basse-
1069 Normandie." Comptes Rendus de l'Académie des Sciences, Paris **115**: 380.
- 1070
- 1071 Bigot, A. (1898). "Feuille des Pieux." Bulletin de la Carte Géologique **63**(Tome X): 1-
1072 7.
- 1073
- 1074 Bigot, A. (1930). "Les terrasses pléistocènes du littoral du Cotentin." Livre Jubilaire
1075 de la Société Géologique de France **tl**: 133-148.
- 1076

- 1077 Bigot, A. (1931). Les terrasses littorales du Cotentin. Congrès International de
1078 Géographie, Paris Librairie Armand Colin.
- 1079
- 1080 Bintanja, R. and R. S. W. Van de Wal (2008). "North American ice-sheet dynamics
1081 and the onset of 100,000-year glacial cycles." Nature **454**(7206): 869-872.
- 1082
- 1083 Bonnet, S., F. Guillocheau, J.-P. Brun and J. Van Den Driessche (2000). "Large
1084 scale relief development related to Quaternary tectonic uplift of a Proterozoic-
1085 Paleozoic basement: The Armorican Massif, NW France." Journal of
1086 Geophysical Research: Solid Earth **105**(B8): 19273-19288.
- 1087
- 1088 Bonow, J. M., P. Japsen, P. F. Green, P. R. Cobbold, A. J. Pedreira, R. Lilletveit and
1089 D. Chiossi (2009). "Post-rift landscape development of north-east Brazil."
1090 Geological Survey of Denmark and Greenland Bulletin **17**: 81-84.
- 1091
- 1092 Bowles, C. J. and E. Cowgill (2012). "Discovering marine terraces using airborne
1093 LiDAR along the Mendocino-Sonoma coast, northern California." Geosphere
1094 **8**(2): 386-402.
- 1095

- 1096 Bradley, W. C. (1957). "Origin of marine terrace deposits in the Santa Cruz area,
1097 California." Bulletin of the Geological Society of America **68**: 421-444.
- 1098
- 1099 Bradley, W. C. and G. B. Griggs (1976). "Form, genesis, and deformation of central
1100 California wave-cut platforms." Geological Society of America bulletin **87**(3):
1101 433-449.
- 1102
- 1103 Brault, N., S. Bourquin, F. Guillocheau, M. P. Dabard, S. Bonnet, P. Courville, J.
1104 Esteoule-Choux and F. Stepanoff (2004). "Mio-Pliocene to Pleistocene
1105 paleotopographic evolution of Brittany (France) from a sequence stratigraphic
1106 analysis: relative influence of tectonics and climate." Sedimentary Geology
1107 **163**(3): 175-210.
- 1108
- 1109 Breton, G., R. Cousin, M.-F. Huault, C. Lechevallier and D. Lefebvre (1991). "Les
1110 sédiments quaternaires du quartier de l'Hôtel de Ville, au Havre : séquences
1111 marines pré-éemienne, éemienne et holocène de l'estuaire de la Seine."
1112 Bulletin trimestrielle de la Société géologique de Normandie et amis du
1113 Muséum du Havre **78**(4): 15-63.
- 1114
- 1115 Breuil, H., M. Vaultier and G. Zbyszewski (1942). "Les Plages anciennes portugaises

- 1116 entre les Caps d'Espichel et Carvoeiro et leurs industries paléolithiques."
- 1117 Bulletin de la Société Préhistorique de France Tome 39(3-4): 93-98.
- 1118
- 1119 Bridgland, D. R. (2002). "Fluvial deposition on periodically emergent shelves in the
1120 Quaternary: example records from the shelf around Britain." Quaternary
1121 International 92(1): 25-34.
- 1122
- 1123 Brodie, J. and N. White (1994). "Sedimentary basin inversion caused by igneous
1124 underplating: Northwest European continental shelf." Geology 22(2): 147-150.
- 1125
- 1126 Bull, A. J. (1941). "Pleistocene chronology." Proceedings of the Geologists'
1127 Association LIII(part I): 1-44.
- 1128
- 1129 Burrough, P. A. and R. A. McDonnell (1998). "Creating continuous surfaces from
1130 point data." Principles of Geographic Information Systems. Oxford University
1131 Press, Oxford, UK.
- 1132
- 1133 Butaeye, D., E. Laville and J. Le Gall (2001). "Géométrie et cinématique des
1134 chevauchements varisques du Nord-Est du Massif armoricain (France)."

- 1135 Comptes Rendus de l'Académie des Sciences - Series IIA - Earth and
1136 Planetary Science **332**(4): 283-289.
- 1137
- 1138 Campar de Almeida, A. (2001). "A carsificacao da serra da Boa Viagem: um
1139 processo Quaternario." Estudos do Quaternario Revista da Associaçao
1140 Portuguesa para o Estudo do Quaternario **4**: 29-33.
- 1141 Caputo, R. (2007). "Sea-level curves: Perplexities of an end-user in morphotectonic
1142 applications." Global and Planetary Change **57**(3-4): 417-423.
- 1143
- 1144 Chambers, R. (1848). Ancient Sea-margins, as memorial of changes in the relative
1145 level of sea and land. Edinburgh, W & R Chambers.
- 1146
- 1147 Clet-Pellerin, M., S. Baize, A.-V. Walter, O. Dugué and J.-P. Coutard (1997). "Mise
1148 en évidence d'un interglaciaire du Pléistocène inférieur dans une formation
1149 fluviatile du Seuil du Cotentin (Normandie, France)." Géographie Physique et
1150 Quaternaire **51**(3): 363-378.
- 1151
- 1152 Cliquet, D. (2015). Les occupations néandertaliennes : des sites spécialisés (250 000
1153 à 40 000 ans) Dans les pas de Néandertal : Les premiers hommes en

- 1154 Normandie de 500 000 à 5 000 ans avant notre ère. S. Berthelot, D. Cliquet
1155 and J.-M. Levesque. Caen, Faton Edition: 84-91.
- 1156
- 1157 Cliquet, D. and J. P. Lautridou (2009). "Les occupations humaines du Pléistocène
1158 moyen de Normandie dans leur cadre environnemental." Quaternaire **20**(3):
1159 305-320.
- 1160
- 1161 Cliquet, D., J. P. Lautridou, M. Lamothe, N. Mercier, J.-L. Schwenninger, P. Alix and
1162 G. Vilgrain (2009). "Nouvelles données sur le site majeur d'Ecalgrain:
1163 Datations radiométriques et occupations humaines de la pointe de la Hague
1164 (Cotentin, Normandie)." Quaternaire **20**(3): 345-359.
- 1165
- 1166 Cliquet, D., N. Mercier, H. Valladas, L. Froget, D. Michel, B. Van Vliet-Lanoë and G.
1167 Vilgrain (2003). "Apport de la thermoluminescence sur silex chauffés à la
1168 chronologie de sites paléolithiques de Normandie : nouvelles données et
1169 interprétations " Quaternaire **14**(1): 51-64.
- 1170
- 1171 Coutard, J.-P. and J. P. Lautridou (1975). "Le Quaternaire de Grandcamp
1172 (Calvados), Loess et plages marines normanniennes: un problème de
1173 datation." Bulletin de la Société Linnéenne de Normandie **104**(136-144).

1174

1175 Coutard, J.-P., J. P. Lautridou, D. Lefebvre and M. Clet (1979). "Les bas-niveaux
1176 marins éemien et pré-éemien de Grandcamp - les - bains." Bulletin de la
1177 Société Linneénne de Normandie **107**: 11-20.

1178

1179 Coutard, S. (2003). Formations quaternaires en bordure d'une mer épicontinentale, la
1180 Manche : tectonique, eustatisme, climat et occupations humaines. Exemple du
1181 Val de Saire (Normandie, France). Caen, Université de Caen: 445.

1182

1183 Coutard, S., J. P. Lautridou and E. Rhodes (2005). "Discontinuités dans
1184 l'enregistrement des cycles glaciaires interglaciaires sur un littoral en contexte
1185 intraplaque, exemple du Val de Saire (Normandie, France) " Quaternaire
1186 **16**(3): 217-227.

1187

1188 Coutard, S., J.-P. Lautridou, E. Rhodes and M. Clet (2006). "Tectonic, eustatic and
1189 climatic significance of raised beaches of Val de Saire, Cotentin, Normandy,
1190 France." Quaternary Science Reviews **25**(5-6): 595-611.

1191

1192 Cunha, L. S., A. A. Martins, J. Cabral, M. P. Gouveia, J.-P. Buylaert and A. S. Murray

- 1193 (2015). Staircases of wave-cut platforms in western central Portugal (Cape
1194 Mondego to Cape Espichel) - relevance as indicators of crustal uplift. VIII
1195 Simposio sobre el Margen Iberico Atlantico, Malaga Centro Oceanografico de
1196 Malaga.
- 1197
- 1198 Cunha, P. P., A. A. Martins, J. Cabral, M. P. Gouveia, J.-P. Buylaert and A. S. Murray
1199 (2015). Escadrias de terraços marinhos em Portugal centro-ocidental -
1200 relevância como indicadores de soerguimento crustal. VOO Congresso
1201 Nacional de Geomorfologia Lisboa
- 1202
- 1203 Daly, R. A. (1925). "Pleistocene changes of level." American Journal of Science - fifth
1204 serie X(58): 281-313
- 1205
- 1206 Davies, B. J., D. R. Bridgland, D. H. Roberts, C. O. Cofaigh, S. M. Pawley, I. Candy,
1207 B. Demarchi, K. E. H. Penkman and W. E. N. Austin (2009). "The age and
1208 stratigraphic context of the Easington Raised Beach, County Durham, UK."
1209 Proceedings of the Geologists' Association **120**(4): 183-198.
- 1210
- 1211 Dawson, A. G., S. Dawson, A. G. Cooper, A. Gemmell and R. Bates (2013). "A
1212 Pliocene age and origin for the strandflat of the Western Isles of Scotland: a

- 1213 speculative hypothesis." Geological Magazine **150**(02): 360-366.
- 1214
- 1215 Depéret, C. (1918-1922). "Essai de coordination chronologique générale des temps
1216 quaternaires : les formations marines " Extraits des Comptes rendus des
1217 séances de l'Académie des Sciences
1218 **166,480,636,884,167,418,979,168,868,873,170,159,171,212,174,1502,1594.**
- 1219
- 1220 Dèzes, P., S. M. Schmid and P. A. Ziegler (2004). "Evolution of the European
1221 Cenozoic Rift System: interaction of the Alpine and Pyrenean orogens with
1222 their foreland lithosphere." Tectonophysics **389**(1): 1-33.
- 1223
- 1224 Døssing, A., P. Japsen, A. B. Watts, T. Nielsen, W. Jokat, H. Thybo and T.
1225 Dahlae• Jensen (2016). "Miocene uplift of the NE Greenland margin linked to
1226 plate tectonics: Seismic evidence from the Greenland Fracture Zone, NE
1227 Atlantic." Tectonics **35** (2) : 257-282
- 1228
- 1229 Dugué, O. (2003). "The Pliocene to Early Pleistocene marine to fluviatile succession
1230 of the Seuil du Cotentin basins (Armorican Massif, Normandy, France)." Journal of Quaternary Science **18**(3-4): 215-226.

1232

1233 Dugué, O., J.-P. Auffret and N. Poupinet (2007). "Cenozoic shelly sands in the
1234 Cotentin (Armorican Massif, Normandy, France): A record of Atlantic
1235 transgressions and intraplate Cenozoic deformations." Comptes Rendus
1236 Geoscience **339**(2): 110-120.

1237

1238 Dugué, O., J. P. Lautridou, F. Quesnel, M. Clet, N. Poupinet and C. Bourdillon
1239 (2009). "Évolution sédimentaire cénozoïque (Paléocène à Pléistocène
1240 inférieur) de la Normandie." Quaternaire **20**(3): 275-303.

1241

1242 Dunlop, A. (1893). "On Raised Beaches and Rolled Stones at High Levels in Jersey."
1243 Quarterly Journal of the Geological Society **49**(1-4): 523-530.

1244

1245 Dupret, L., E. Dissler, F. Doré, F. Gresselin and J. Le Gall (1990). "Cadomian
1246 geodynamic evolution of the northeastern Armorican Massif (Normandy and
1247 Maine)." Geological Society, London, Special Publications **51**(1): 115-131.

1248

1249 Dutton, A., E. Bard, F. Antonioli, T. M. Esat, K. Lambeck and M. T. McCulloch (2009).
1250 "Phasing and amplitude of sea-level and climate change during the

- 1251 penultimate interglacial." Nature Geosciences **2**(5): 355-359.
- 1252
- 1253 Elhaï, H. (1960). "A propos des niveaux marins quaternaires en Normandie." Bulletin
1254 de la Société Linnéenne de Normandie **1**: 137-145.
- 1255
- 1256 Ferreira Soares, A. (1999). "As unidades Pliocenicas e Quaternarias no espaço do
1257 baixo Mondego (uma perspectiva de ordem)." Estudos do Quaternario Revista
1258 da Associação Portuguesa para o Estudo do Quaternario **2**: 7-17.
- 1259
- 1260 Ferreira Soares, A., P. M. Callapez and J. Fonseca Marques (2007). "The Farol
1261 deposit (deposito do Farol) - a pleistocene beach deposit from Cape Mondego
1262 (Figueira da Foz, West Central Portugal)." Ciencias da Terra (UNL) **16**: 163-
1263 173.
- 1264
- 1265 Figueiredo, P. M., J. Cabral and T. K. Rockwell (2011). Plio-Pleistocene tectonic
1266 activity in the Southwest of Portugal. 2nd INQUA - IGCP 567 International
1267 workshop on Active Tectonics, Earthquake Geology, Archealogy and
1268 engineering, Corinth, Greece.
- 1269

- 1270 Fleury, L., J.-P. Clément, F. o. Ménillet, G. Moguedet, C. Vinchon and G. Farjanel
1271 (1989). "Les sables rouges et graviers des plateaux et des karsts du Maine
1272 méridional; Etude sédimentologique." Géologie de la France **1**(2): 255-257.
- 1273
- 1274 Font, M., J.-L. Lagarde, D. Amorese, J.-P. Coutard and J.-C. Ozouf (2002). "Une
1275 méthode de quantification de la dégradation d'un escarpement de faille au
1276 cours des cycles climatiques du Quaternaire : la faille de Jobourg (Nord
1277 Cotentin, France)." Comptes Rendus Geoscience **334**(3): 171-178.
- 1278
- 1279 Frankel, K. L. and J. F. Dolan (2007). "Characterizing arid region alluvial fan surface
1280 roughness with airborne laser swath mapping digital topographic data."
1281 Journal of Geophysical Research: Earth Surface **112**(F2).
- 1282
- 1283 Garcin, M., G. Farjanel, S. Courbouleix, P. Barrier, P. Braccini, G. Brébion, R. P.
1284 Carbonel, J. C. Carriol and M. Clet-Pellerin (1997). "La longue séquence
1285 Pliocène de Marchésieux -résultats analytiques et premiers résultats "
1286 Géologie de la France **3**: 39-77.
- 1287
- 1288 Gautier, M. (1967). "La tectonique tertiaire dans le massif Armorican." Annales de
1289 Géographie **414**: 168-197.

1290

1291 Gibbard, P.L. (1988). "The history of the great northwest European rivers during the
1292 past three million years". Philosophical Transactions of the Royal Society of
1293 London, Series B **318**: 559-602

1294

1295 Gonzalez-Acebron, L., R. Mas, J. Arribas, J. M. Gutierrez-Mas and C. Perez-Garrido
1296 (2016). "Very coarse-grained beaches as a response to generalized sea level
1297 drops in a complex active tectonic setting: Pleistocene marine terraces at the
1298 Cadiz coast, SW Spain." Marine Geology **382**(Supplement C): 92-110.

1299

1300 Graindor, M. J. (1964). "Le Quaternaire marin de Normandie." Bulletin de la Société
1301 Géologique de Normandie et des Amis du Muséum du Havre **54**: 1-15.

1302

1303 Grant, K. M., E. J. Rohling, C. B. Ramsey, H. Cheng, R. L. Edwards, F. Florindo, D.
1304 Heslop, F. Marra, A. P. Roberts and M. E. Tamisiea (2014). "Sea-level
1305 variability over five glacial cycles." Nature communications **5**(5076).

1306

1307 Green, P. F., I. R. Duddy, P. Japsen, J. M. Bonow and J. A. Malan (2016). "Post-
1308 breakup burial and exhumation of the southern margin of Africa." Basin

1309 Research. **29** (1): 96-127

1310

1311 Gresselin, F. (2000). Evolution varisque du Massif armoricain oriental : insertion dans
1312 une transversale ouest-européenne. Ecole de Géologie Structurale Caen,
1313 University of Caen: 335 p.

1314

1315 Guilcher, A. (1949). "Aspects et problèmes morphologiques du massif de Devon-
1316 Cornwall comparés à ceux d'Armorique." Revue de Géographie Alpine **37**(4):
1317 689-717.

1318

1319 Guilcher, A. (1951). "La formation de la mer du Nord, du Pas-de-Calais et des
1320 plaines maritimes environnantes." Revue de géographie de Lyon **26**(3): 311-
1321 329.

1322

1323 Guilcher, A. (1969). "Pleistocene and Holocene sea level changes " Earth Sciences
1324 Review **5**: 69-97.

1325

1326 Guilcher, A. (1974). "Les «rasas» : un problème de morphologie littorale générale."
1327 Annales de Géographie **83**(455): 1-33.

1328

1329 Guilcher, A. and B. Hallegouet (1981). "Le haut cordon de galets Pléistocène de
1330 Ruvein en Plovan (Finistère) et ses enseignements généraux." Bulletin de
1331 l'Association Française pour l'Etude du Quaternaire **18**(6): 75-82.

1332

1333 Guillocheau, F., N. Brault, E. Thomas, J. Barbarand, S. Bonnet, S. Bourquin, J.
1334 Estéoule-Choux, P. Guennoc, D. Menier, D. Néraudeau, J.-N. Proust and R.
1335 Wyns (2003). "Histoire géologique du Massif Armorican depuis 140 Ma
1336 (Crétacé-Actuel)." Bulletin Information Géologique du Bassin de Paris **40**(1):
1337 13-28.

1338

1339 Hallégouët, B. (1976). "Les anciens dépôts marins et fluviatiles de la vallée de l'Elorn
1340 (Finistère)" Norois **89**: 55-72.

1341

1342 Hamblin, R.J.O. Crosby, A. Balson, P.S. Jones, S.M. Chadwick, R.A., Penn I.E.,
1343 Arthur M.J. (1992). The Geology of the English Channel. United Kingdom
1344 Offshore Regional Report, British Geological Survey. HMSO: London; 106 pp

1345

1346 Home, H. (1912). "Worked flints obtained from the 25-foot raised beach near

- 1347 Holywood, co. Down." Nature **224**(90): 361.
- 1348
- 1349 Husson, L., P. Yamato and A. Bézos (2015). "Ultraslow, slow, or fast spreading
1350 ridges: Arm wrestling between mantle convection and far-field tectonics."
1351 Earth and Planetary Science Letters **429**: 205-215.
- 1352
- 1353 Japsen, P., J. Bonow, P. Green, J. Chalmers and K. Lidmar- Bergström (2006).
1354 "Elevated, passive continental margins: Long-term highs or Neogene uplifts?
1355 New evidence from West Greenland." Earth and Planetary Science Letters
1356 **248**: 330-339.
- 1357
- 1358 Japsen, P., J. M. Bonow, P. F. Green, P. R. Cobbold, D. Chirossi, R. Lilletveit, L. P.
1359 Magnavita and A. Pedreira (2012). "Episodic burial and exhumation in NE
1360 Brazil after opening of the South Atlantic." Geological Society of America
1361 Bulletin **124**(5-6): 800-816.
- 1362
- 1363 Japsen, P. and J. A. Chalmers (2000). "Neogene uplift and tectonics around the
1364 North Atlantic: overview." Global and Planetary Change **24**(3): 165-173.
- 1365

- 1366 Jara-Muñoz, J. and D. Melnick (2015). "Unraveling sea-level variations and tectonic
1367 uplift in wave-built marine terraces, Santa María Island, Chile." Quaternary
1368 Research **83**(1): 216-228.
- 1369
- 1370 Jara-Muñoz, J., D. Melnick and M. R. Strecker (2016). "TerraceM: A MATLAB® tool
1371 to analyze marine and lacustrine terraces using high-resolution topography."
1372 Geosphere **12**(1): 176-195.
- 1373
- 1374 Jara-Muñoz J, Melnick D, Zambrano P, Rietbrock A, González J, Argandoña B,
1375 Strecker MR. (2017): "Quantifying offshore forearc deformation and splay-fault
1376 slip using drowned Pleistocene shorelines, Arauco Bay, Chile". Journal of
1377 Geophysical Research, Solid Earth, **122** (6) 4529–4558.
- 1378
- 1379 Jardine, W. G. (1981). "The determination of former shoreline positions in areas of
1380 large tidal range, with examples taken mainly from Scotland." Bulletin de
1381 l'Association française pour l'étude du quaternaire **18**(2): 67-70.
- 1382
- 1383 Juignet, P. (1980). "Transgressions-régressions, variations eustatiques et influences
1384 tectoniques de l'Aptien au Maastrichtien dans le Bassin de Paris occidental et
1385 sur la bordure du Massif armoricain." Cretaceous Research **1**(4): 341-357.

1386

1387 Klein (1975). "Massif armoricain et Bassin parisien." Fondation Baulig Vol 2

1388

1389 Kopp, R. E., F. J. Simons, J. X. Mitrovica, A. C. Maloof and M. Oppenheimer (2009).

1390 "Probabilistic assessment of sea level during the last interglacial stage."

1391 Nature **462**(7275): 863-867.

1392

1393 Lagarde, J. L., D. Amorese, M. Font, E. Laville and O. Dugué (2003). "The structural

1394 evolution of the English Channel area." Journal of Quaternary Science **18**(3-

1395 4): 201-213.

1396

1397 Lagarde, J.-L., S. Baize, D. Amorese, B. Delcaillau, M. Font and P. Volant (2000).

1398 "Active tectonics, seismicity and geomorphology with special reference to

1399 Normandy (France)." Journal of Quaternary Science **15**(7): 745-758.

1400

1401 Lajoie, K. R. (1986). Coastal Tectonics. Active tectonic. N. A. Press. Washington

1402 D,C, National Academic Press: 95-124.

1403

- 1404 Lajoie, K. R., D. J. Ponti, C. L. Powell, A. M. Mathieson and A. M. Sarna - Wojcicki
1405 (1991). Emergent marine strandlines and associated sediments, coastal
1406 California: a record of Quaternary sea-level fluctuations, vertical tectonic
1407 movements, climatic changes, and coastal processes. Quaternary Nonglacial
1408 Geology: Conterminous U.S.: The Geology of North America. Morrison.
1409 Boulder, Colorado, Geological Society of America. **K-2**: 190-214.
- 1410
- 1411 Lambeck, K. (1991). "Glacial rebound and sea-level change in the British Isles."
1412 Terra Nova **3**(4): 379-389.
- 1413
- 1414 Lambeck, K. (1996). "Glaciation and sea-level change for Ireland and the Irish Sea
1415 since Late Devensian/Midlandian time." Journal of the Geological Society
1416 **153**(6): 853-872.
- 1417
- 1418 Larroueur, C., R. Horn, J. P. Auffret, P. Hommeril and A. Moal (1975). "Geologie de
1419 la Partie Meridionale de la Manche Centrale." Philosophical Transactions of
1420 the Royal Society of London A: Mathematical, Physical and Engineering
1421 Sciences **279**(1288): 145-153.
- 1422
- 1423 Lautridou, J. P. (1983). Le Quaternaire de Normandie. Caen, Centre de

- 1424 Géomorphologie du CNRS.
- 1425
- 1426 Lautridou, J. P. (1985). Le cycle périgaciaire pléistocène en Europe du Nord-Ouest et
1427 plus particulièrement en Normandie. Centre de Géomorphologie du CNRS.
1428 Caen, University of Caen. **Doctorat d'état:** 970.
- 1429
- 1430 Lautridou, J. P. (1989). "Les lignes de rivages Pléistocènes en Normandie âge des
1431 plates-formes littorales." Bulletin du Centre de Géomorphologie du CNRS.
1432 Caen **36:** 231-234.
- 1433
- 1434 Lautridou, J. P., S. Baize, M. Clet, J.-P. Coutard and J.-C. Ozouf (1999). "Les
1435 séquences plio-pléistocènes littorales et estuariennes de Normandie."
1436 Quaternaire **10**(2-3): 161-169.
- 1437
- 1438 Leorri, E., F. Fatela, T. Drago, S. L. Bradley, J. Moreno and A. Cearreta (2012).
1439 "Lateglacial and holocene coastal evolution of the Minho estuary (N Portugal) :
1440 implications for understanding sea-level changes in Atlantic Iberia." The
1441 Holocene **23**(3): 353-363.
- 1442

- 1443 Lericolais, G., J.-P. Auffret and J.-F. Bourillet (2003). "The Quaternary Channel River:
1444 seismic stratigraphy of its palaeo-valleys and deeps." Journal of Quaternary
1445 Science **18**(3-4): 245-260.
- 1446
- 1447 Lisiecki, L. E. and M. E. Raymo (2005). "A Pliocene-Pleistocene stack of 57 globally
1448 distributed benthic delta ^{18}O records." Paleoceanography **20**: PA1003.
- 1449
- 1450 Lyell, C. (1830). Principles of geology, being an attempt to explain the former
1451 changes of the earth's surface, by reference to causes now in operation.
1452 London, John Murray.
- 1453
- 1454 Mellett, C. L., D. M. Hodgson, A. J. Plater, B. Mauz, I. Selby and A. Lang (2013).
1455 "Denudation of the continental shelf between Britain and France at the
1456 glacialâ€“interglacial timescale." Geomorphology **203**: 79-96.
- 1457
- 1458 Melnick, D. (2016). "Rise of the central Andean coast by earthquakes straddling the
1459 Moho." Nature Geoscience.**9**: 401-416.
- 1460
- 1461 Miller, K. G., M. A. Kominz, J. V. Browning, J. D. Wright, G. S. Mountain, M. E. Katz,

- 1462 P. J. Sugarman, B. S. Cramer, N. Christie-Blick and S. F. Pekar (2005). "The
1463 Phanerozoic record of global sea-level change." science **310**(5752): 1293-
1464 1298.
- 1465
- 1466 Milne, G. A., A. J. Long and S. E. Bassett (2005). "Modelling Holocene relative sea-
1467 level observations from the Caribbean and South America." Quaternary
1468 Science Reviews **24**(10-11): 1183-1202.
- 1469
- 1470 Moore, D. (1842). "On fossil bones found on the surface of a raised beach at the
1471 Hoe, near Plymouth." Transactions of the Geological Society **IV**(3rd series):
1472 97-98.
- 1473
- 1474 Moreno, F. and J. Mediato (2009). Terrazas del rio Miera. Difluencia durante su
1475 desarrollo (Cantabria). 6 Simposio sobre el Margen Iberico Atlantico, Oviedo
- 1476
- 1477 Murray-Wallace, C. and C. Woodroffe (2014). Quaternary sea level : a global
1478 perspective. Cambridge, Cambridge University Press.
- 1479
- 1480 Nexer, M. (2015). Etudes conjointe des réseaux de drainage et des paléocôtes plio-

- 1481 quaternaires soulevées:exemples de l'Indonésie et du Golfe Normand Breton.
- 1482 Caen, University of Caen. **PhD:** 374 pp
- 1483 Oliva (1977). "La plateforme Moghrébienne : néotectonique et eustatisme sur le
1484 littoral de l'Anti-Atlas." **Méditerranée Deuxième série, Tome 29(2):** 73-91.
- 1485
- 1486 Pareyn, C. (1980). "Mise en évidence d'une activité néotectonique pliocène et
1487 quaternaire dans le Cotentin, le bassin de Carentan et le Bessin (Manche et
1488 Calvados)." **Bulletin de la Société Géologique de France tome XXII(4):** 695-
1489 701.
- 1490
- 1491 Paskoff, R. and P. Sanlaville (1983). "Les côtes de la Tunisie, variations du niveau
1492 marin depuis le tyrrhénien. Travail réalisé dans le cadre de l'ERA 345 du
1493 CNRS " **Collection de la Maison de l'Orient Méditerranéen : Série**
1494 **Géographique et Préhistorique:** 190.
- 1495
- 1496 Pedoja, K., J. F. Dumont, M. Lamothe, L. Ortlieb, J.-Y. Collot, B. Ghaleb, M. Auclair,
1497 V. Alvarez and B. Labrousse (2006) a. "Plio-Quaternary uplift of the Manta
1498 Peninsula and La Plata Island and the subduction of the Carnegie Ridge,
1499 central coast of Ecuador." **Journal of South American Earth Sciences 22(1-2):**
1500 1-21.

- 1501 Pedoja, K., L. Ortlieb, J. F. Dumont, M. Lamothe, B. Ghaleb, M. Auclair and B.
1502 Labrousse (2006) b. "Quaternary coastal uplift along the Talara Arc (Ecuador,
1503 Northern Peru) from new marine terrace data." Marine Geology **228**(1-4): 73-
1504 91.
- 1505
- 1506 Pedoja, K., L. Husson, V. Regard, P. R. Cobbold, E. Ostanciaux, M. E. Johnson, S.
1507 Kershaw, M. Saillard, J. Martinod, L. Furgerot, P. Weill and B. Delcaillau
1508 (2011). "Relative sea-level fall since the last interglacial stage: Are coasts
1509 uplifting worldwide?" Earth-Science Reviews **108**(1-2): 1-15.
- 1510
- 1511 Pedoja, K., L. Husson, M. E. Johnson, D. Melnick, C. Witt, S. Pochat, M. Nexer, B.
1512 Delcaillau, T. Pinegina, Y. Poprawski, C. Authemayou, M. Elliot, V. Regard
1513 and F. Garestier (2014). "Coastal staircase sequences reflecting sea-level
1514 oscillations and tectonic uplift during the Quaternary and Neogene." Earth-
1515 Science Reviews **132**(0): 13-38.
- 1516
- 1517 Pellerin, J., P. Brebion, M. Helluin, J.-T. Hollin, A. Lauriat - Rage, D. Lefévre and G.
1518 H. Miller (1987). "Données nouvelles sur le gisement marin Quaternaire +
1519 14.5/15.7 m NGF du cimetière de Luc sur mer (Calvados, France)." Bulletin du
1520 Centre de Géomorphologie du CNRS, Caen **32**(99-115).

- 1521
- 1522 Pellerin, J. and P. A. Dupeuble (1979). "Le bas niveau marin Eemien de Graye-sur-
1523 Mer (Calvados)." Bulletin Société Linnéene de Normandie **107**: 21-26.
- 1524
- 1525 Peulvast, J.-P., V. C. Sales, F. o. Bâtard and Y. Gunnell (2008). "Low post-
1526 Cenomanian denudation depths across the Brazilian Northeast: implications
1527 for long-term landscape evolution at a transform continental margin." Global
1528 and Planetary Change **62**(1): 39-60.
- 1529
- 1530 Prestwich, J. (1851). "On the Drift at Sangatte Cliff, near Calais." Quarterly Journal of
1531 the Geological Society **7**(1-2): 274-278.
- 1532
- 1533 Prestwich, J. (1862-1863). "Theoretical considerations on the condition under which
1534 the drift deposits containing the remains of extinct mammalia and flint-
1535 implements were accumulated : and on their geological age." Proceedings of
1536 the Royal Society of London **12**: 38-52.
- 1537
- 1538 Prestwich, J. (1865). "Additional Observations on the Raised Beach of Sangatte with
1539 reference to the Date of the English Channel, and the Presence of Loess in

- 1540 the Cliff Section." Quarterly Journal of the Geological Society **21**(1-2): 440-
- 1541 442.
- 1542
- 1543 Prestwich, J. (1892). "The Raised Beaches, and 'Head' or Rubble-drift, of the South
1544 of England: their Relation to the Valley Drifts and to the Glacial Period; and on
1545 a late post-Glacial Submergence." Quarterly Journal of the Geological Society
1546 **48**(1-4): 263-343.
- 1547
- 1548 Quezada, J., G. Gonzalez, T. Dunai, A. Jensen and J. Juez-Larré (2007).
1549 "Alzamiento litoral Pleistoceno del norte de Chile: edades 21Ne de la terraza
1550 costera más alta del área de Caldera-Bahía Inglesa." Revista Geológica de
1551 Chile **34**(1): 81-96.
- 1552
- 1553 Ramos, A. M. and P. P. Cunha (2009). O Pliocenico e o Plistocenico da plataforma
1554 litoral entre os paralelos da Serra da Boa Viagem e da Nazaré (Portugal
1555 central). 6e simposio sobre a margem iberico atlantica, Oviedo.
- 1556
- 1557 Ramos, A. M., P. P. Cunha, L. S. Cunha, A. Gomes, F. C. Lopes, J.-P. Buylaert and
1558 A. S. Murray (2012). "The River Mondego terraces at the Figueira da Foz
1559 coastal area (western central Portugal): geomorphological and

- 1560 sedimentological characterization of a terrace staircase affected by differential
1561 uplift and glacio eustasy " Geomorphology **165-166**: 107-123.
- 1562
- 1563 Ramos, A. M., P. P. Cunha, A. Gomes and L. S. Cunha (2010). Caracterização
1564 geomorfologica e sedimentologica da escadaria de terraços da margem direita
1565 do rio Mondego, no sector entre Maiorca e Vila Verde. VI Seminario Latino
1566 Americano de Geografia Fisica II Seminario Ibero Americano de Geografia
1567 Fisica Coimbra, Universidad de Coimbra.
- 1568
- 1569 Raynal, J.-P., D. Lefevre, D. Geraads and M. El Graoui (1999). "Contribution du site
1570 paléontologique de Lissasfa (Casablanca, Maroc) à une nouvelle
1571 interprétation du Mio-Pliocène de la Méseta." Comptes Rendus de l'Académie
1572 des Sciences-Series IIA-Earth and Planetary Science **329**(8): 617-622.
- 1573
- 1574 Regard, V., M. Saillard, J. Martinod, L. Audin, S. Carretier, K. Pedoja, R. Riquelme,
1575 P. Paredes and G. Hérail (2010). "Renewed uplift of the Central Andes
1576 Forearc revealed by coastal evolution during the Quaternary." Earth and
1577 Planetary Science Letters **297**(1-2): 199-210.
- 1578
- 1579 Regnault, H., B. Mauz and M.-T. Morzadec-Kerfourn (2003). "The last interglacial

- 1580 shoreline in northern Brittany, western France." Marine Geology **194**(1-2): 65-
- 1581 77.
- 1582
- 1583 Renouf, J. and L. James (2011). "High level shore features of Jersey (Channel Islands) and adjacent areas." Quaternary International **231**(1-2): 62-77.
- 1584
- 1585
- 1586 Roberts, G. P., M. Meschis, S. Houghton, C. Underwood and R. M. Briant (2013).
- 1587 "The implications of revised Quaternary palaeoshoreline chronologies for the
- 1588 rates of active extension and uplift in the upper plate of subduction zones."
- 1589 Quaternary Science Reviews **78**: 169-187.
- 1590
- 1591 Rohling, E. J., G. L. Foster, K. M. Grant, G. Marino, A. P. Roberts, M. E. Tamisiea
- 1592 and F. Williams (2014). "Sea-level and deep-sea-temperature variability over
- 1593 the past 5.3 million years." Nature **508**(7497): 477-482.
- 1594
- 1595 Rohling, E. J., K. Grant, M. Bolshaw, A. P. Roberts, M. Siddall, C. Hemleben and M.
- 1596 Kucera (2009). "Antarctic temperature and global sea level closely coupled
- 1597 over the past five glacial cycles." Nature Geosciences **2**: 500-504.
- 1598

- 1599 Rosenbaum, G., G. S. Lister and C. Duboz (2002). "Relative motions of Africa, Iberia
1600 and Europe during Alpine orogeny." Tectonophysics **359**(1-2): 117-129.
- 1601
- 1602 Sanlaville, P. (1974). "Le rôle de la mer dans les aplatissements côtiers du Liban."
1603 Revue de géographie de Lyon **49**(4): 295-310.
- 1604
- 1605 Scuvée, F. and D. Alduc (1981). "Deux niveaux marins Pléistocènes et leurs
1606 industries paléolithiques respectives sur le littoral du Cotentin (Manche)."
1607 Bulletin de la Société préhistorique française **tome 78**: 210-218.
- 1608
- 1609 Shakun, J. D., D. W. Lea, L. E. Lisiecki and M. E. Raymo (2015). "An 800-kyr record
1610 of global surface ocean $\delta^{18}\text{O}$ and implications for ice volume-temperature
1611 coupling." Earth and Planetary Science Letters **426**: 58-68.
- 1612
- 1613 Shennan, I. and B. Horton (2002). "Holocene land- and sea-level changes in Great
1614 Britain." Journal of Quaternary science **17**(5-6): 511-526.
- 1615
- 1616 Sheppard, G. (1927). "Geological observations on Isla de la Plata, Ecuador, South
1617 America." American Journal of Science **13**: 480-486.

1618

1619 Sheppard, G. (1930). "The geology of southwestern Ecuador." American Association
1620 of Petroleum Geologist Bulletin **14**: 263-309.

1621

1622 Siddall, M., J. Chappell and E.-K. Potter (2006). Eustatic sea level during past
1623 interglacials. The Climate of Past Interglacials. F. Sirocko, M. Claussen, M. F.
1624 Sanchez Goñi and T. Litt. Amsterdam, Elsevier: 75-92.

1625

1626 Siddall, M., E. J. Rohling, A. Almogi-Labin, C. Hemleben, D. Meischner, I. Schmelzer
1627 and D. A. Smeed (2003). "Sea-level fluctuations during the last glacial cycle."
1628 Nature **423**(6942): 853-858.

1629

1630 Silva, C., B. Landau, R. Domènech and J. Martinelli (2010). "Pliocene Atlantic
1631 molluscan assemblages from the Mondego Basin (Portugal):age and
1632 palaeoceanographic implications." Palaeogeography, Palaeoclimatology,
1633 Palaeoecology **285**: 248-254.

1634

1635 Sommé, J. and P. Antoine (1989). "La plaine maritime de la mer du Nord (France) et
1636 le pas de Calais : du Pléistocène moyen à l'Holocène." Bulletin du Centre de

- 1637 Géomorphologie du CNRS, Caen **36**: 219-222.
- 1638
- 1639 Sommé, J., P. Antoine, N. Cunat-Bogé, D. Lefèvre and A. V. Munaut (1999). "The
1640 marine middle pleistocene of the north sea in France : Sangatte cliff and
1641 Herzeele formation." Quaternaire **10**(2-3): 151-160.
- 1642
- 1643 Spratt, R. M. and L. E. Lisiecki (2016). "A Late Pleistocene sea level stack." Climate
1644 of the Past **12**(4): 1079.
- 1645
- 1646 Stirling, C. H., T. M. Esat, K. Lambeck and M. T. McCulloch (1998). "Timing and
1647 duration of the Last Interglacial: evidence for a restricted interval of
1648 widespread coral reef growth." Earth and Planetary Science Letters **160**(3-4):
1649 745-762.
- 1650
- 1651 Stirling, C. H., T. M. Esat, K. Lambeck, M. T. McCulloch, S. G. Blake, D.-C. Lee and
1652 A. N. Halliday (2001). "Orbital Forcing of the Marine Isotope Stage 9
1653 Interglacial." Science **291**(5502): 290-293.
- 1654
- 1655 Sutcliffe, A. J., A. P. Curran and C. B. Stringer (1987). "Evidence of sea-level

- 1656 change from coastal caves with raised beach deposits, terrestrial faunas and
1657 dated stalagmites." Progress in oceanography **18**(1-4): 243-271.
- 1658
- 1659 Szabo, B. J. and J. G. Vedder (1971). "Uranium-series dating of some pleistocene
1660 marine deposits in southern California." Earth and Planetary Science Letters
1661 **11**: 283-290.
- 1662
- 1663 Teixeira, C. (1944). "Tectonica Plio-Pleistonica do Noroeste Peninsular." Boletim da
1664 Sociedade Geológica de Portugal **Vol. IV**(Fasc. I-II): 19-40.
- 1665
- 1666 Teixeira, C. (1948). "Les dépôts modernes du littoral portugais au Nord de Leiria."
1667 Boletim da Sociedade Geológica de Portugal **Vol. VII**(Fasc. I-II): 83-94.
- 1668
- 1669 Telfer, M., J. L. Schwenninger, R. T. Walker, R. A. Sloan, A. B. Watts, R. L. Kahle, B.
1670 Kahle and M. W. Dee (2016). "Rapid mantle-driven uplift along the Angolan
1671 margin in the late Quaternary." Nature Geoscience **9**: 909-914.
- 1672
- 1673 Tessier, B., N. Delsinne and P. Sorrel (2013). "Holocene sedimentary infilling of a
1674 tide-dominated estuarine mouth. The example of the macrotidal Seine estuary

- 1675 (NW France)." Bulletin de la Societe Geologique de France **181**(2): 87-98.
- 1676
- 1677 Texier, J.-P. and J. Meireles (1987). "As formações Quaternárias do Litoral do Minho
1678 (Portugal): propostas para uma nova abordagem climato-cronológica e
1679 dinâmica." Cadernos de Arqueologia Serie II(4): 9-33.
- 1680
- 1681 Thompson, W. G. and S. L. Goldstein (2005). "Open-system coral ages reveal
1682 persistent suborbital sea-level cycles." Science **308**(5720): 401-404.
- 1683
- 1684 Thompson, W. G., M. W. Spiegelman, S. L. Goldstein and R. C. Speed (2003). "An
1685 open-system model for U-series age determinations of fossil corals." Earth
1686 and Planetary Science Letters **210**(1-2): 365-381.
- 1687
- 1688 van de Plassche, O. (1986). Sea-level research : a manual for the collection and
1689 evaluation of data. Norwich, UK, Geo Books.
- 1690
- 1691 van Vliet-Lanoë, B., M. Laurent, J. L. Bahain, S. Balescu, C. Falguères, M. Field, B.
1692 Hallégouët and D. H. Keen (2000). "Middle Pleistocene raised beach
1693 anomalies in the English Channel: regional and global stratigraphic

- 1694 implications." Journal of Geodynamics **29**(1-2): 15-41.
- 1695
- 1696 van Vliet-Lanoë, B., N. Vandenberghe, M. Laurent, B. Laignel, A. Lauriat-Rage, S.
- 1697 Louwey, J.-L. Mansy, D. Mercier, B. Hallegouet, F. Meilliez, Y. Michel, G.
- 1698 Moguedet and J.-P. Vidier (2002). "Palaeogeographic evolution of
- 1699 northwestern Europe during the Upper Cenozoic." Geodiversitas **24**(3): 511-
- 1700 541.
- 1701
- 1702 Vérague, J. (1983). "Le gisement sablo-graveleux cénozoïque probable du hameau
- 1703 du Cloquant (La Glacerie, Normandie)." Norois **118**: 293-302.
- 1704
- 1705 Waelbroeck, C., L. D. Labeyrie, E. Michel, J. C. Duplessy, J. F. McManus, K.
- 1706 Lambeck, E. Balbon and M. Labracherie (2002). "Sea-level and deep water
- 1707 temperature changes derived from benthic foraminifera isotopic records."
- 1708 Quaternary Science Reviews **21**: 295-305.
- 1709
- 1710 Westaway, R. (1993). "Quaternary uplift of Southern Italy." Journal of Geophysical
- 1711 Research **98**(B12): 21 741-21 772.
- 1712

- 1713 Westaway, R. (2009). "Quaternary uplift of northern England." Global and Planetary
1714 Change **68**: 357-382.
- 1715
- 1716 Whittow, J. B. (1960). "Some comments on the raised beach platform of South West
1717 Caernarvonshire and on an unrecorded raised beach at Porth Neigwl, North
1718 Wales." Proceedings of the Geologist's Association **71**: 31-39.
- 1719
- 1720 Wythe Cooke, C. (1930). "Correlation of coastal terraces." The Journal of Geology
1721 **XXXVIII**(7): 577-589.
- 1722
- 1723 Yamato, P., L. Husson, T. W. Becker and K. Pedoja (2013). "Passive margins getting
1724 squeezed in the mantle convection vice." Tectonics **32**(6): 2013TC003375.
- 1725
- 1726 Yildirim, C., D. Melnick, P. Ballato, T. F. Schildgen, H. Echtler, A. E. Erginal, N. G. n.
1727 Käyak and M. R. Strecker (2013). "Differential uplift along the northern margin
1728 of the Central Anatolian Plateau: inferences from marine terraces." Quaternary
1729 Science Reviews **81**(0): 12-28.
- 1730
- 1731 Zachos, J. C., G. R. Dickens and R. E. Zeebe (2008). "An early Cenozoic perspective

- 1732 on greenhouse warming and carbon-cycle dynamics." Nature **451**(7176): 279-
- 1733 283.
- 1734
- 1735 Zazo, C., P. G. Silva, J. L. Goy, C. Hillaire Marcel, B. Ghaleb, J. Lario, T. Bardaji and
- 1736 A. Gonzalez (1999). "Coastal uplift in continental collision plate boundaries:
- 1737 data from the last interglacial marine terrace of the Gibraltar Strait area (South
- 1738 Spain)." Tectonophysics **301**: 95-109.
- 1739
- 1740 Ziegler, P. A. and P. Dèzes (2007). "Cenozoic uplift of Variscan Massifs in the Alpine
- 1741 foreland: Timing and controlling mechanisms." Global and Planetary Change
- 1742 **58**(1-4): 237-269.
- 1743

Table 1

Area	Site	Terrace	Chrono-stratigraphy	Dating Method	Reference	Elevations						Age MIS	
						Elevation of deposits / Landform		Elevation Strandline / NGF		Elevation Strandline / landform			
						Ed	MoE	Es	MoE	Es	MoE	age	MoE
East	Anse du Brick, Fermanville - Port Levy, Anse de Quéry	T1	MIS 5e	5 OSL dating	Coutard, 2003; Coutard et al., 2005; 2006	*	*	7	1	5	1	122	6
West	Herquemoulin	T1	MIS 5e	Palynology	Clet, 1983	2	1	7	1	5	1	122	6
	Cap de la Hague	T1	MIS 5e	morphostratigraphy	this study	*	*	7	1	5	1	122	6

Table 2

Terrace	Chrono-stratigraphy	Elevation Strandline / NGF		Elevation Strandline / landform		Age MIS		Apparent uplift	
		Es	MoE	Es	MoE	age	MoE	U max	U min
T1	MIS 5e	7	1	5	1	122	6	0.05	0.03
T2	MIS 7	15	2	12	2	217.5	27.5	0.07	0.04
T3	MIS 9	25	3	22	3	324.5	18.5	0.08	0.06
T4	MIS 11	33	3	29	3	390	30	0.09	0.06

Table 3

		Elevation		Apparent MIS 5e uplift rates				Corre
				U maximum	U minimum	U mean		
		0.05	0.03	0.04		0.04		0.12
		E	Moe	minimum extrapolated age	maximum extrapolated age	mean extrapolated age	mean extrapolated age error	minimum extrapolated age
rasa 1	distal	54	5	980	1967	1473	493	408
	proximal	86	5	1620	3033	2327	707	675
rasa 2	distal	95	5	1800	3333	2567	767	750
	proximal	138	5	2660	4767	3713	1053	1108
rasa 3	distal	148	5	2860	5100	3980	1120	1192
	proximal	165	5	3200	5667	4433	1233	1333
rasa 4	distal	172	5	3340	5900	4620	1280	1392
	proximal	185	10	3500	6500	5000	1500	1458

Table 4

MIS	Uplift rate (mm/yr)	Highstand (ka)	sea level corrected to (m)	calculated expected IE (m)	Measured IE (m)	Terrace allocation
5c	0.01	100	-25	-24	-20	offshore
5e	0.01	125	5	6	5	T1
6d	0.01	175	-30	-28		
7a	0.01	200	-5	-3		
7c	0.01	217	-30	-28		
7e	0.01	240	-5	-3		
9a	0.01	285	-30	-27		
9c	0.01	310	-22	-19		
9e	0.01	340	5	8	12	T2
11c	0.01	410	-5	-1		
13a	0.01	478	0	6		
13c	0.01	525	20	25	22	T3
15a (?)	0.01	550	10	16		
15a (?)	0.01	560	3	9		
15c	0.01	590	20	26		
15e	0.01	620	20	26		
17c	0.01	695	10	17		
?	0.01	740	5	12		
19c?	0.01	800	20	28		
21a?	0.01	855	20	29		
?	0.01	980	25	35	33	T4

Figure (Color)

[Click here to download high resolution image](#)

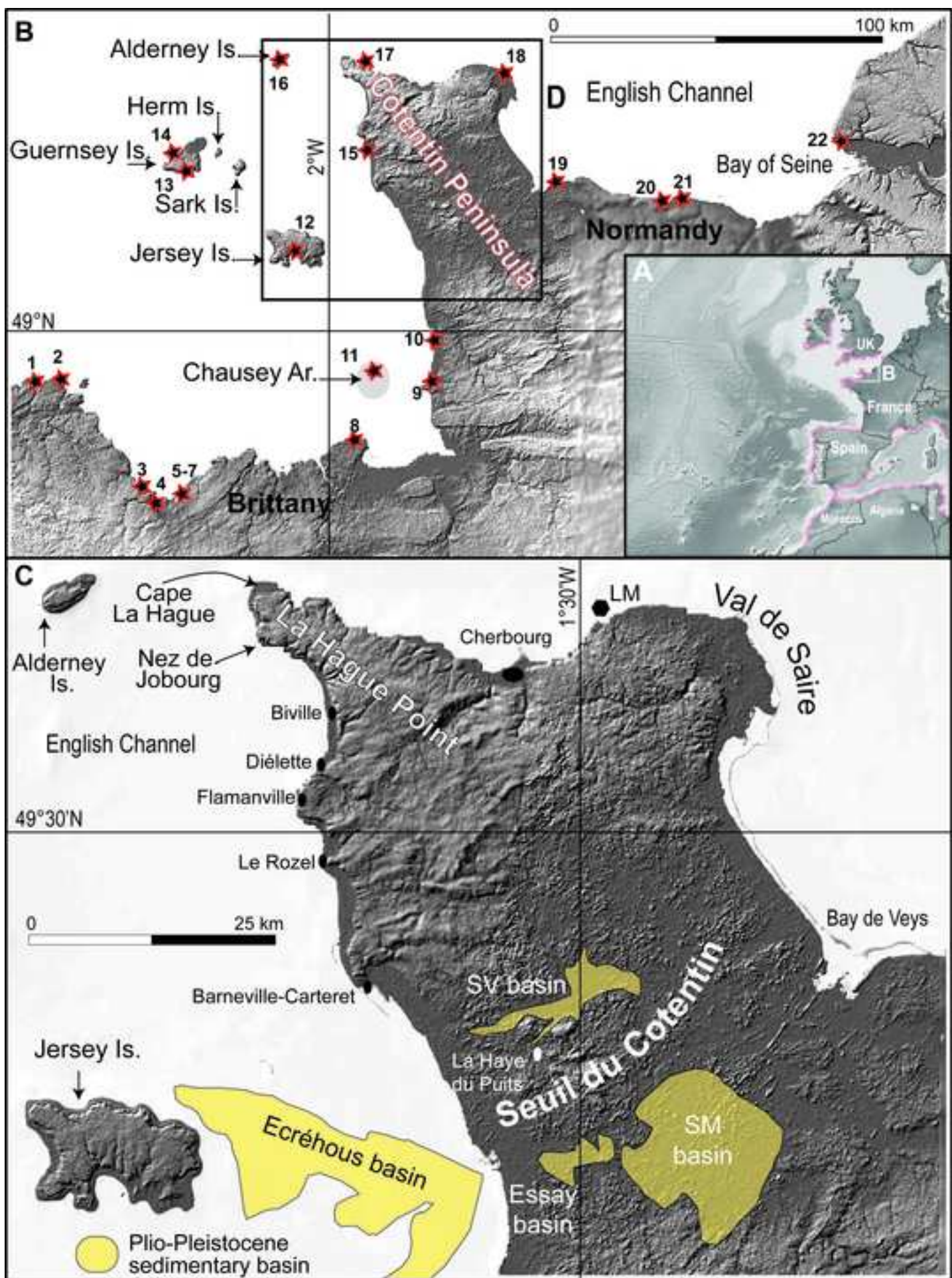


Figure 2 (Color)

[Click here to download high resolution image](#)

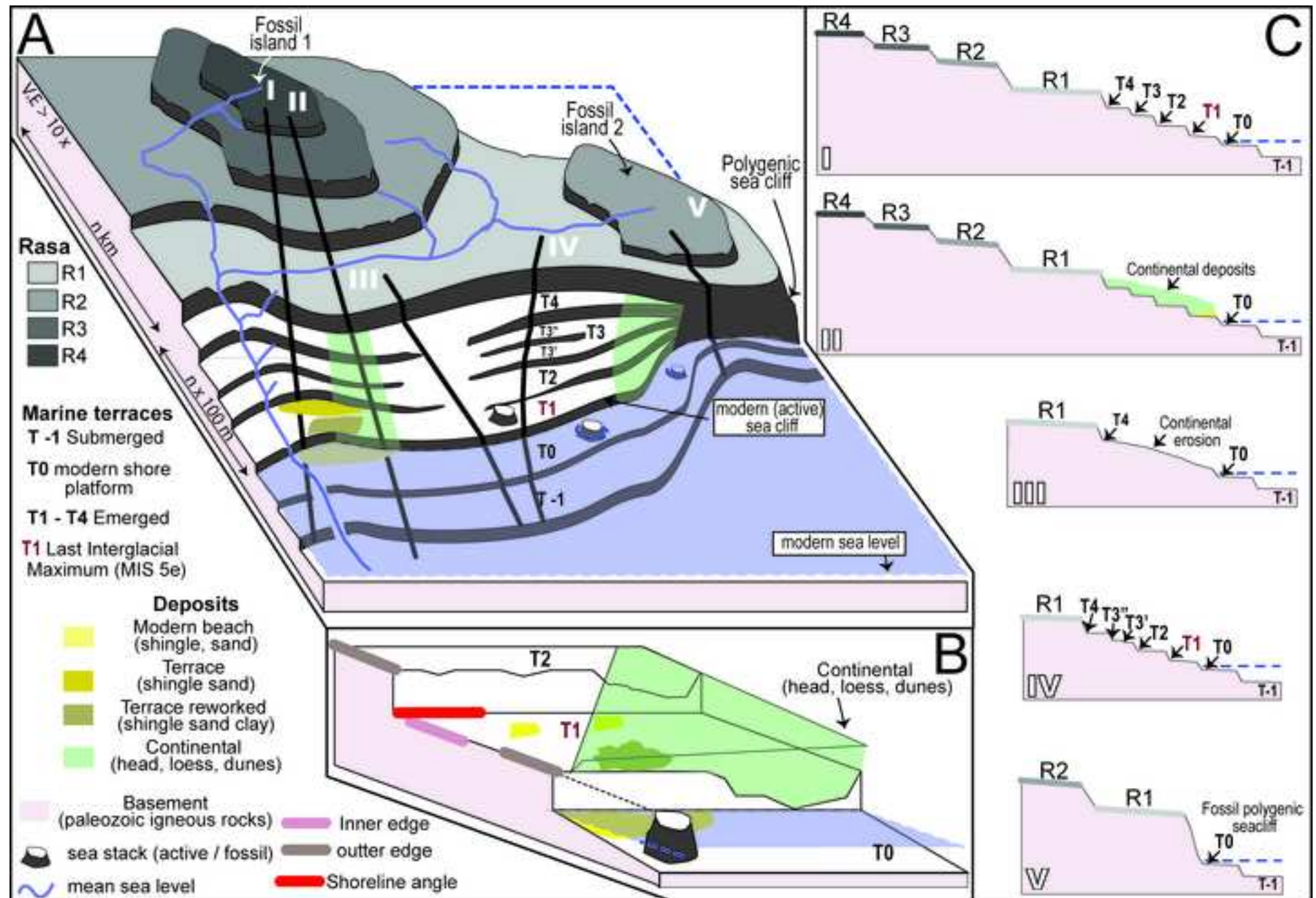


Figure 3 (Color)

[Click here to download high resolution image](#)

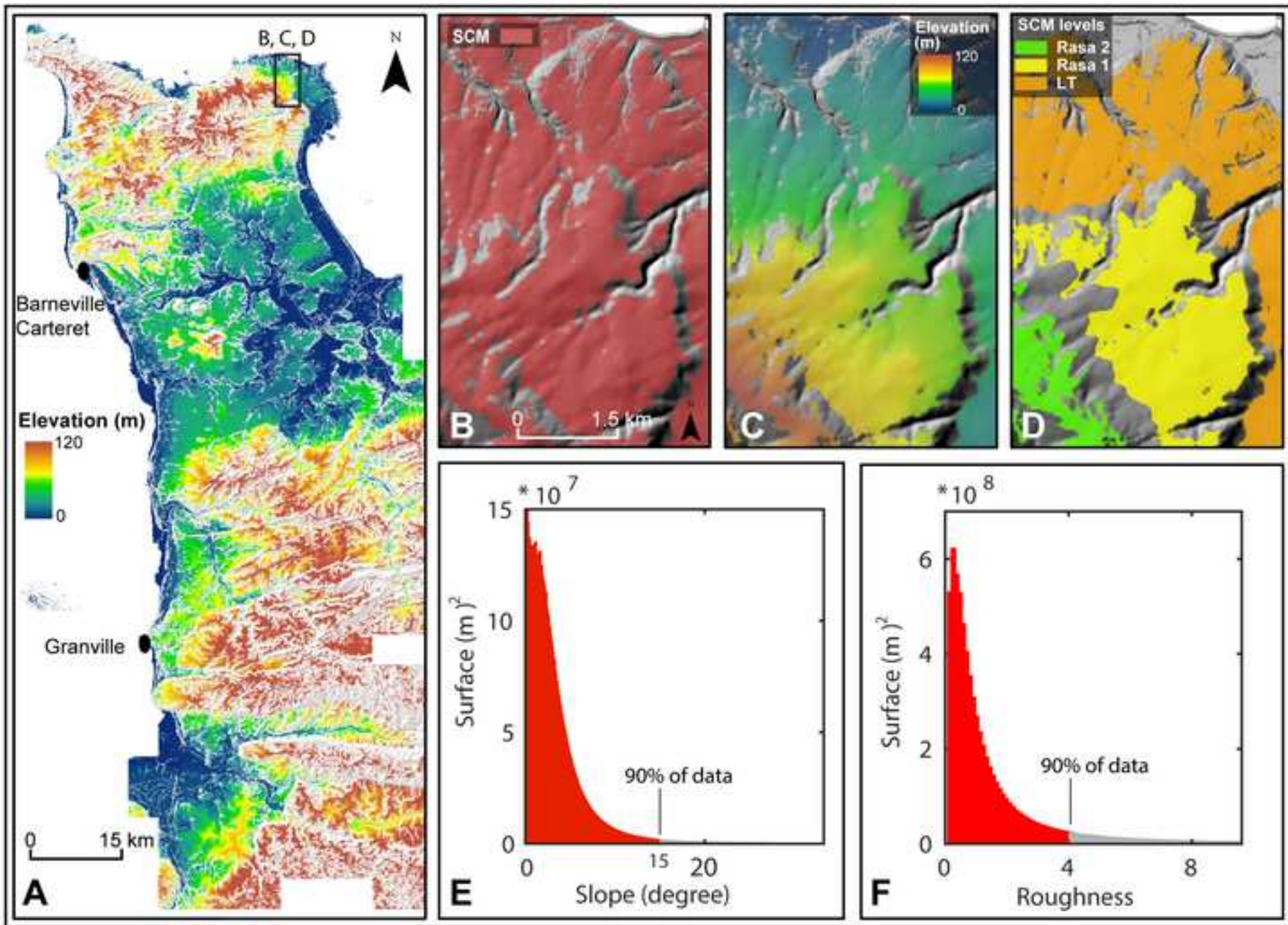


Figure 4 (Color)

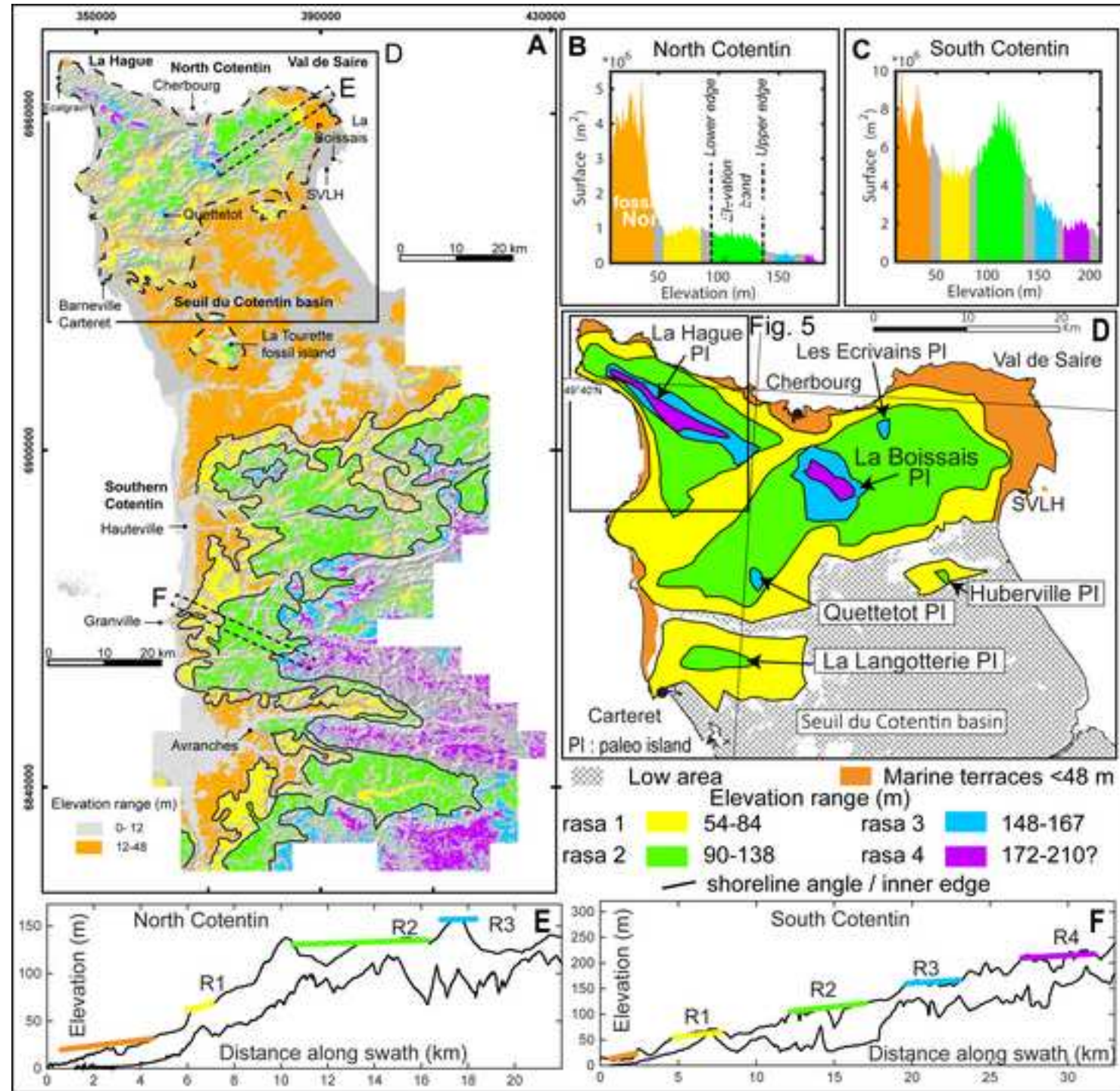
[Click here to download high resolution image](#)

Figure 5 (Color)

[Click here to download high resolution image](#)

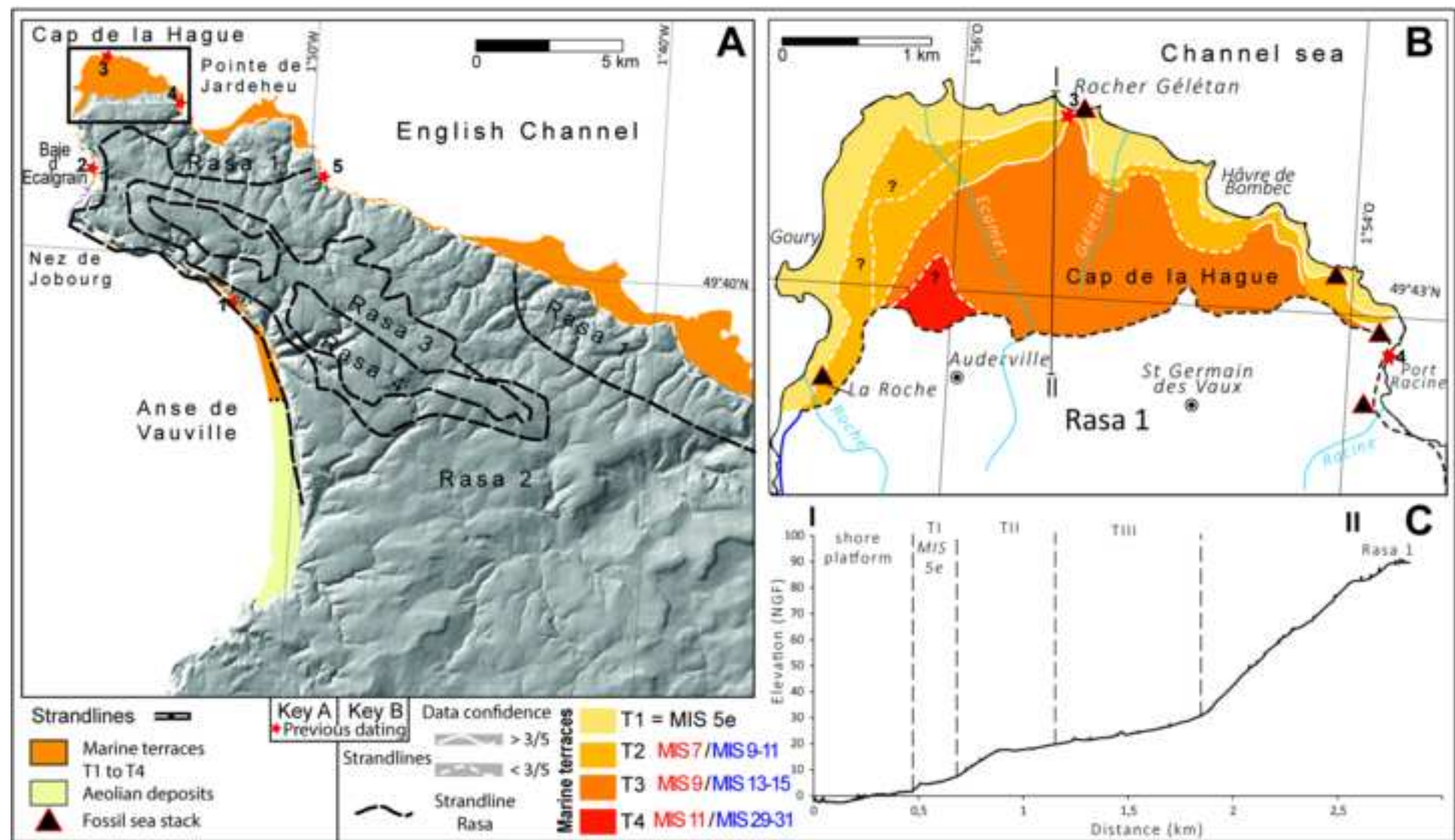


Figure 6 (Color)

[Click here to download high resolution image](#)

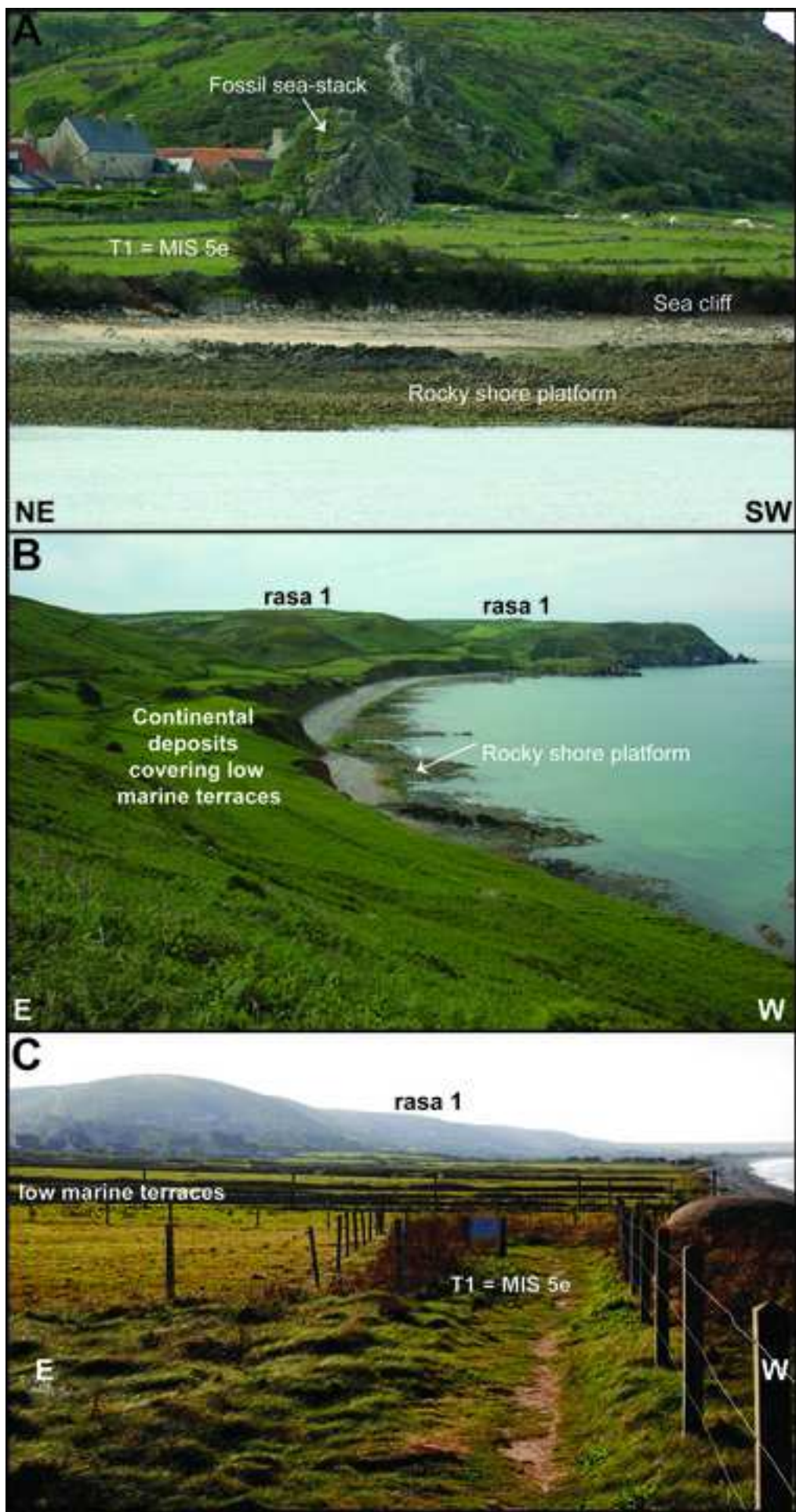


Figure 7 (Color)

[Click here to download high resolution image](#)

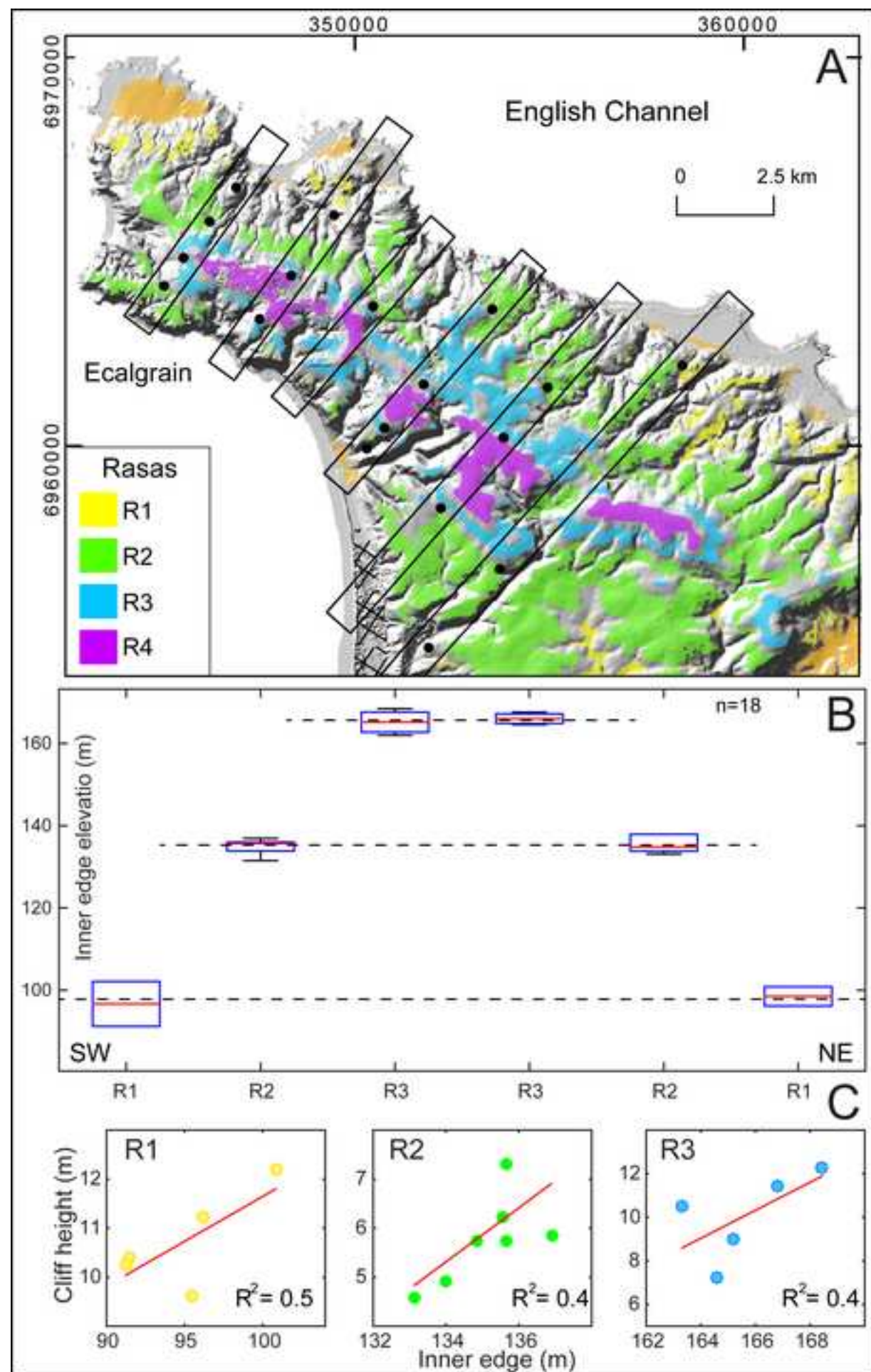


Figure 8 (Color)

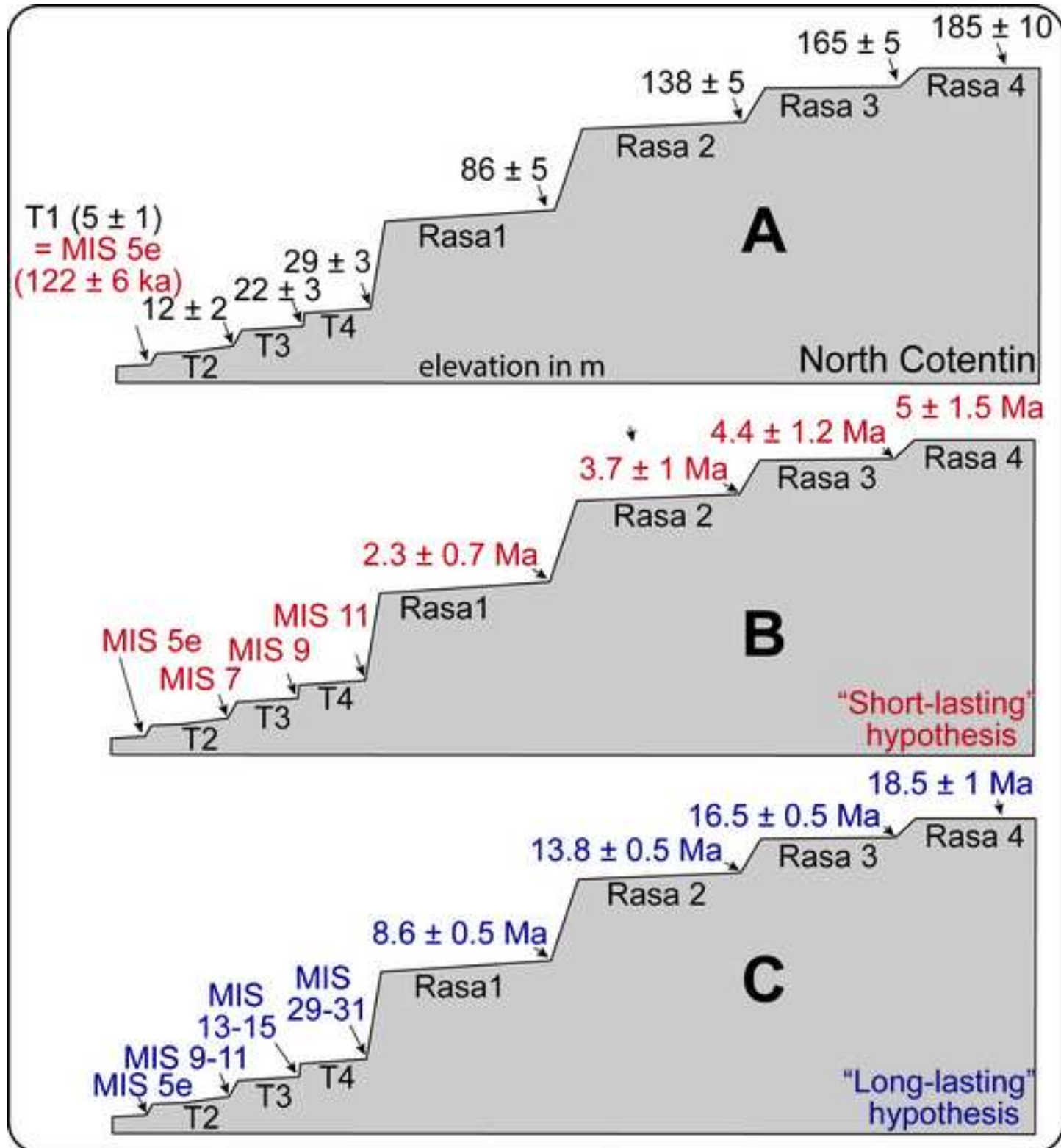
[Click here to download high resolution image](#)

Figure 9 (Color)

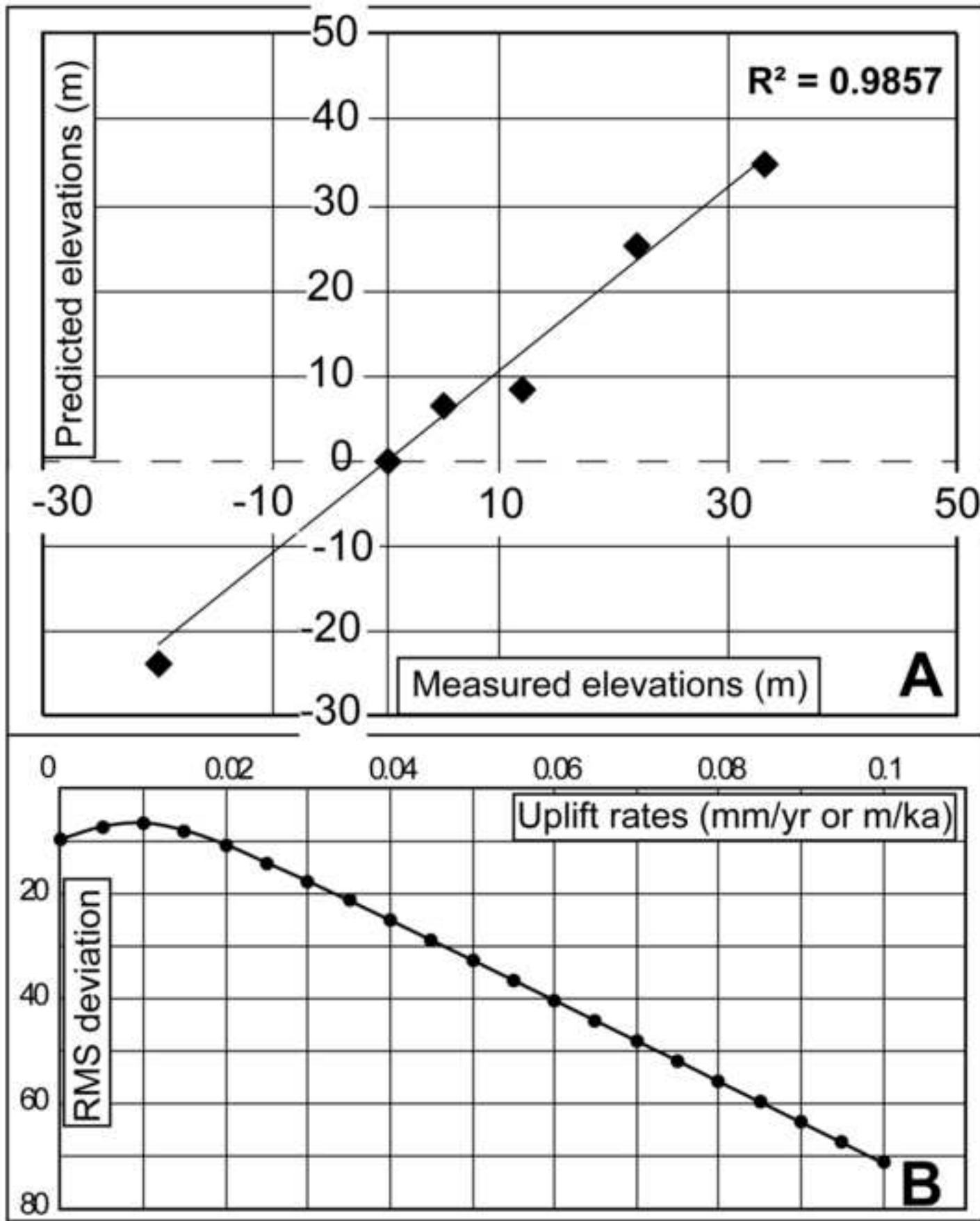
[Click here to download high resolution image](#)

Figure (Color) 10

[Click here to download high resolution image](#)

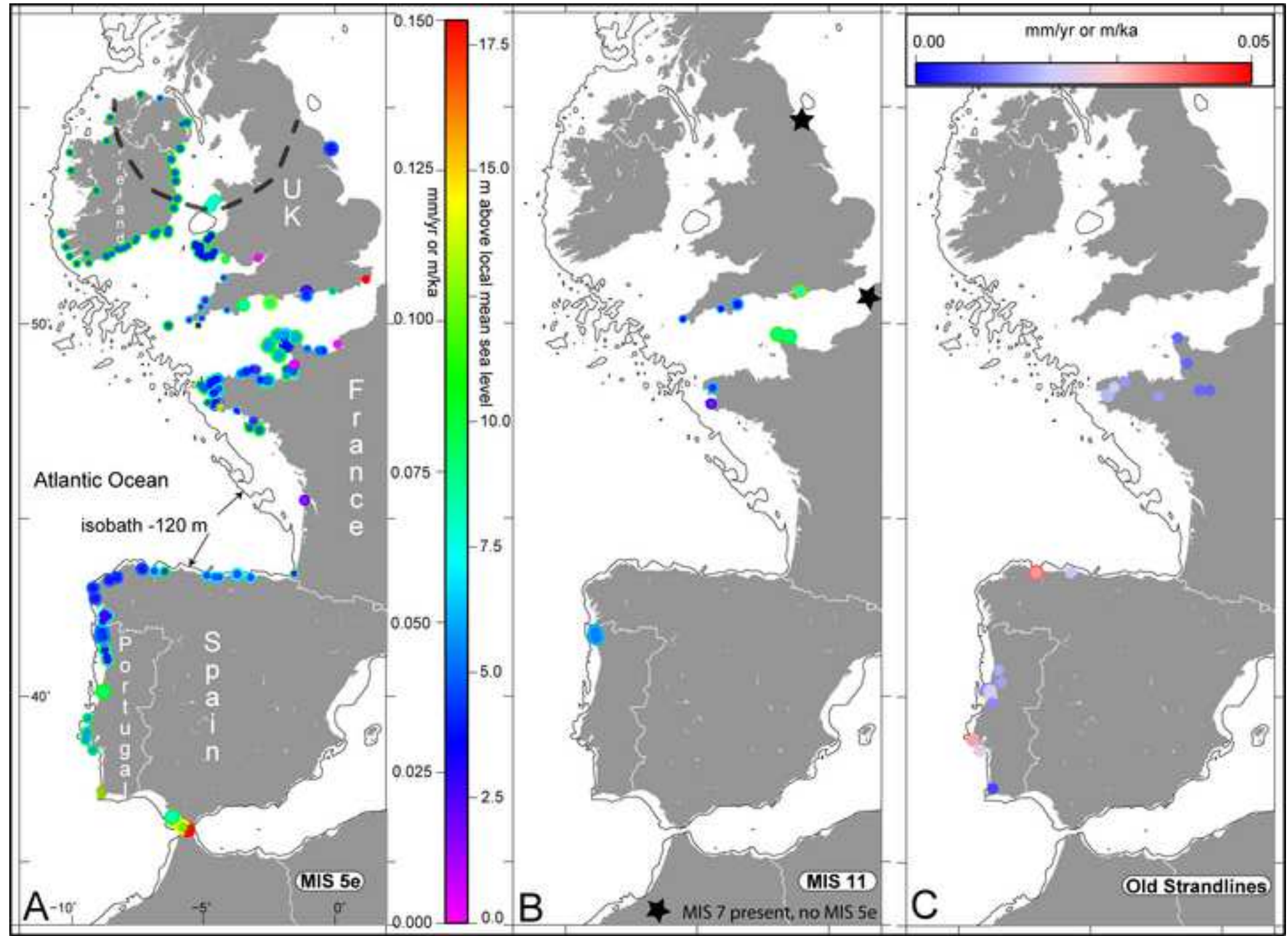


Figure 1 (Greyscale)

[Click here to download high resolution image](#)

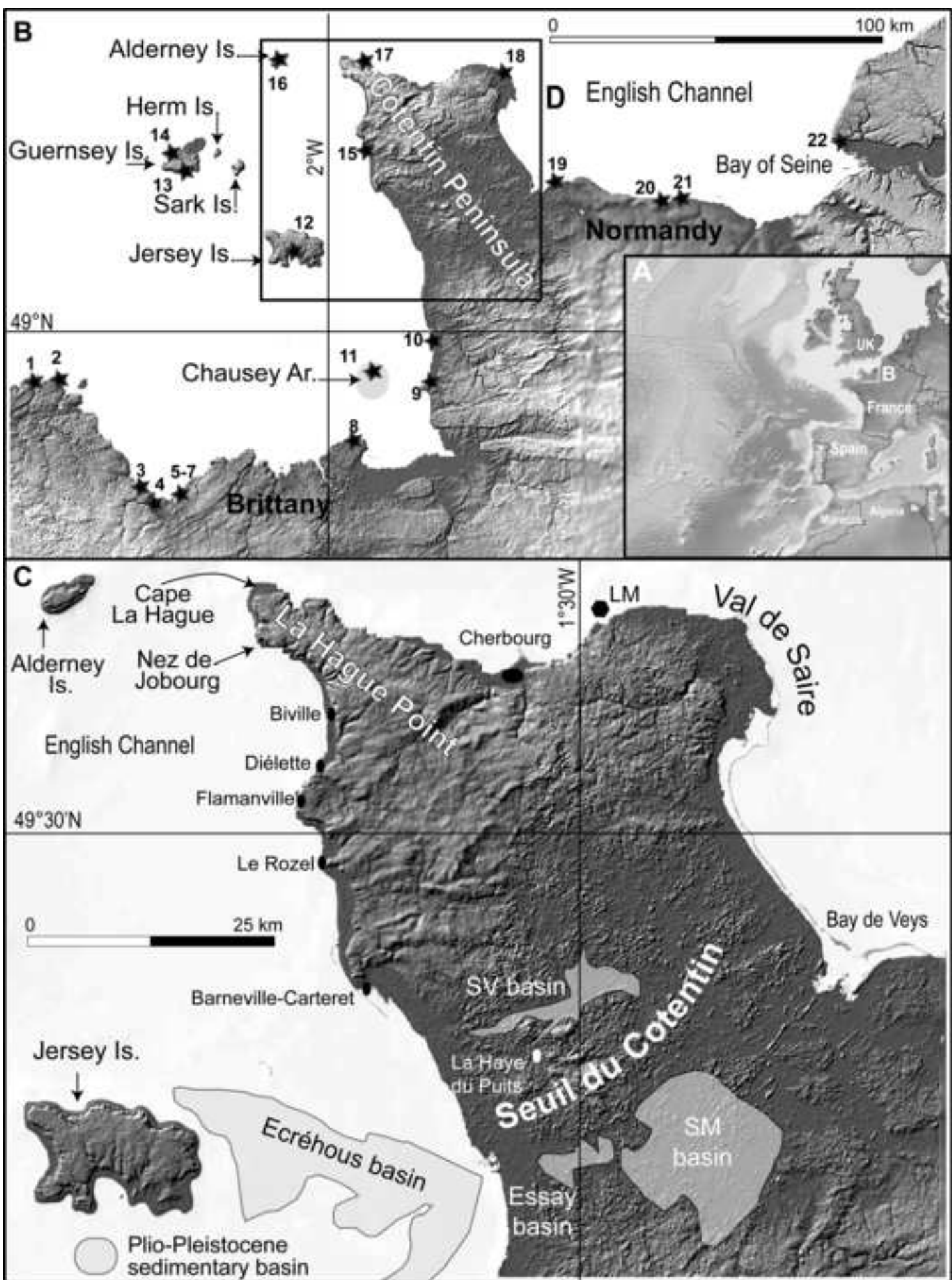


Figure 2 (Greyscale)

[Click here to download high resolution image](#)

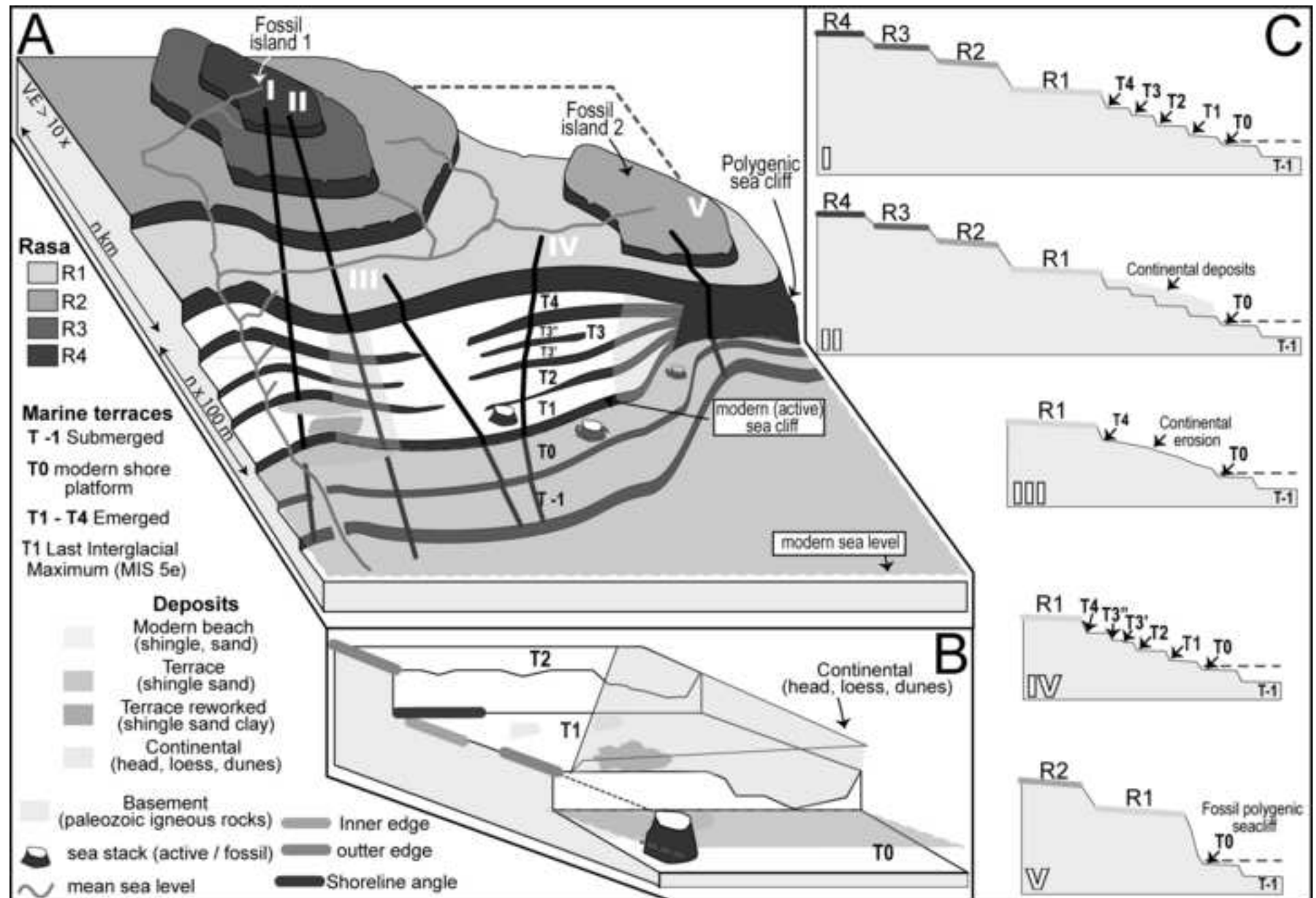


Figure 3 (Greyscale)

[Click here to download high resolution image](#)

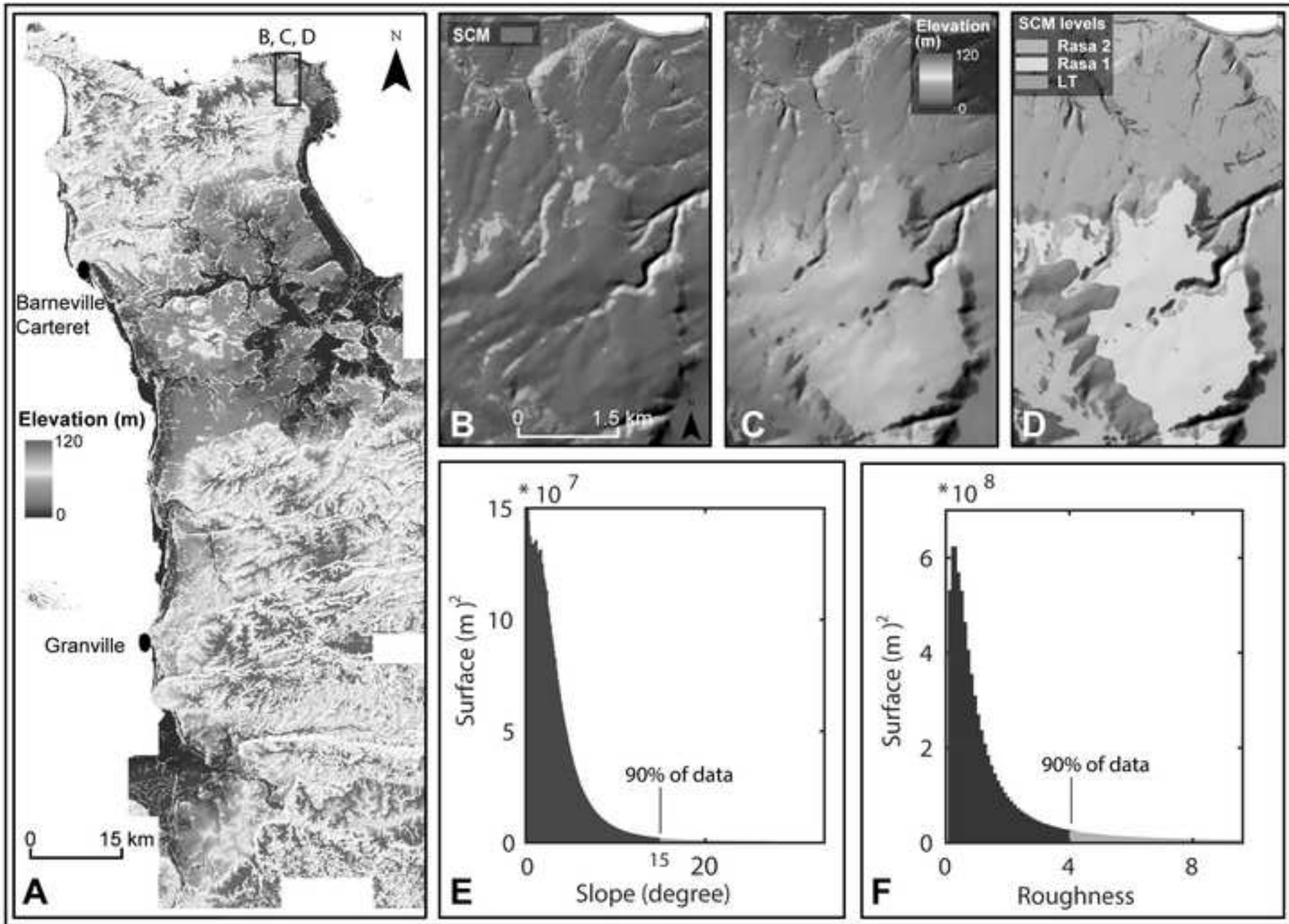


Figure 4 (Greyscale)

[Click here to download high resolution image](#)

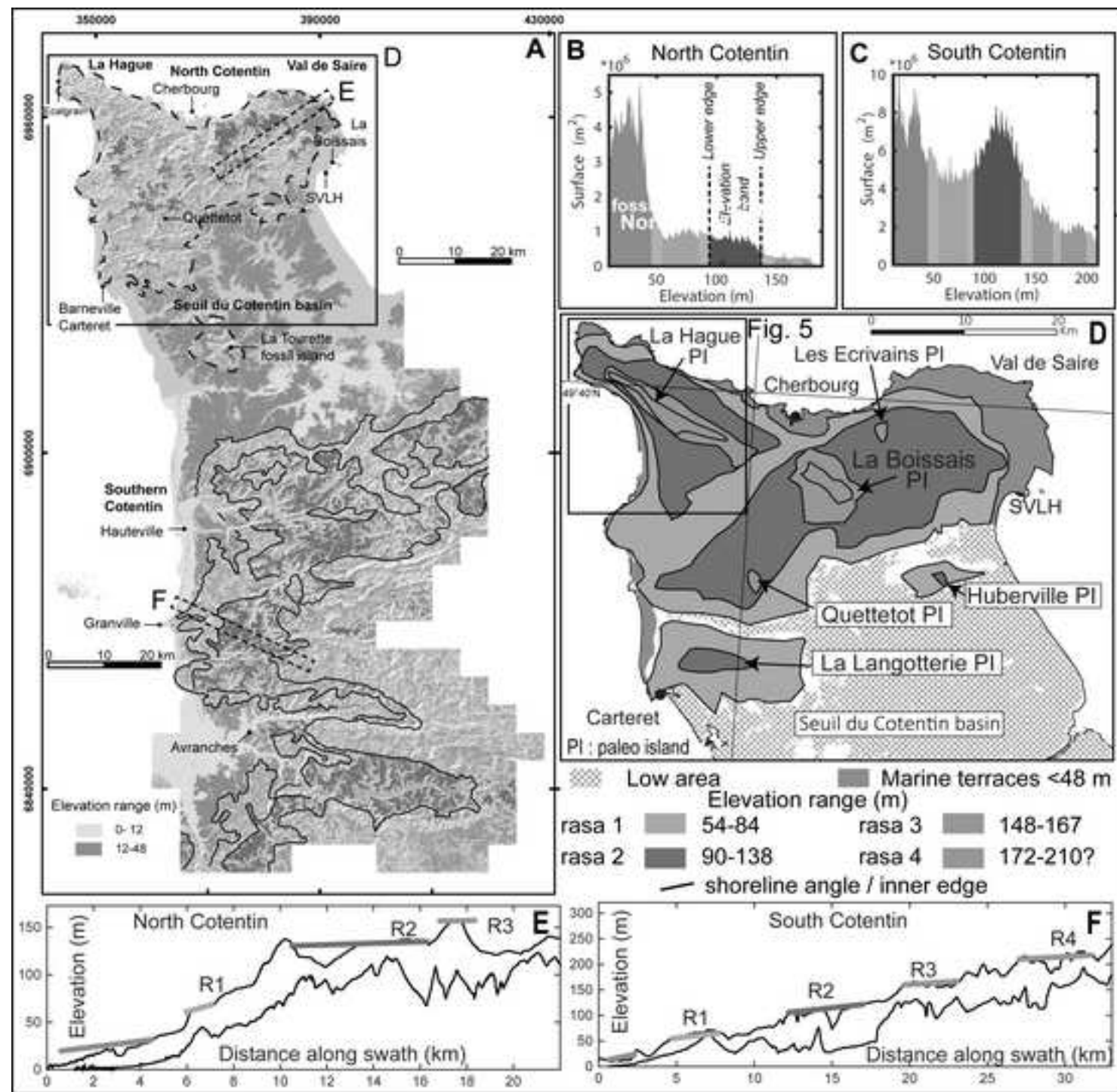


Figure 5 (Greyscale)

[Click here to download high resolution image](#)

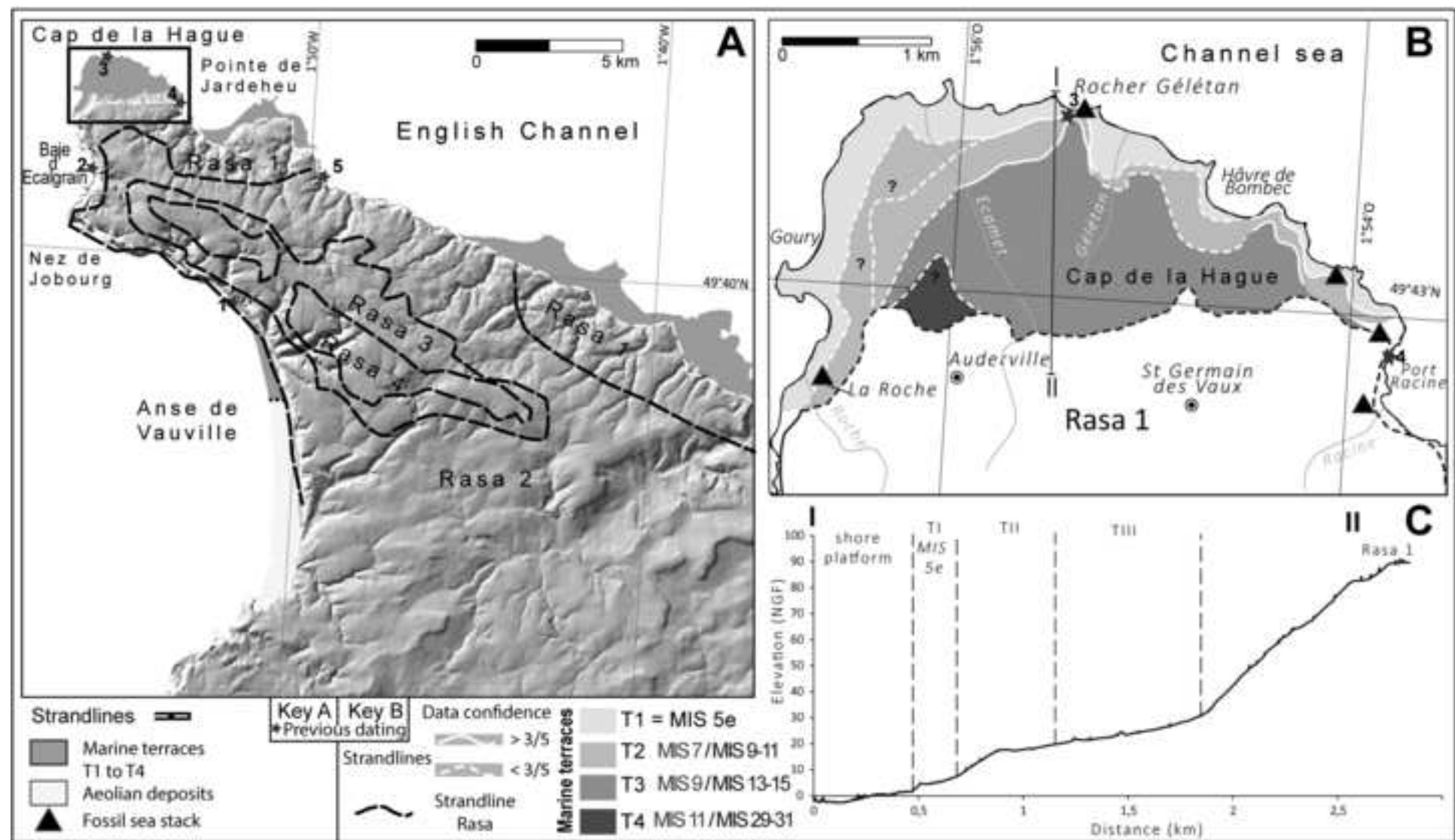


Figure 6 (Greyscale)

[Click here to download high resolution image](#)

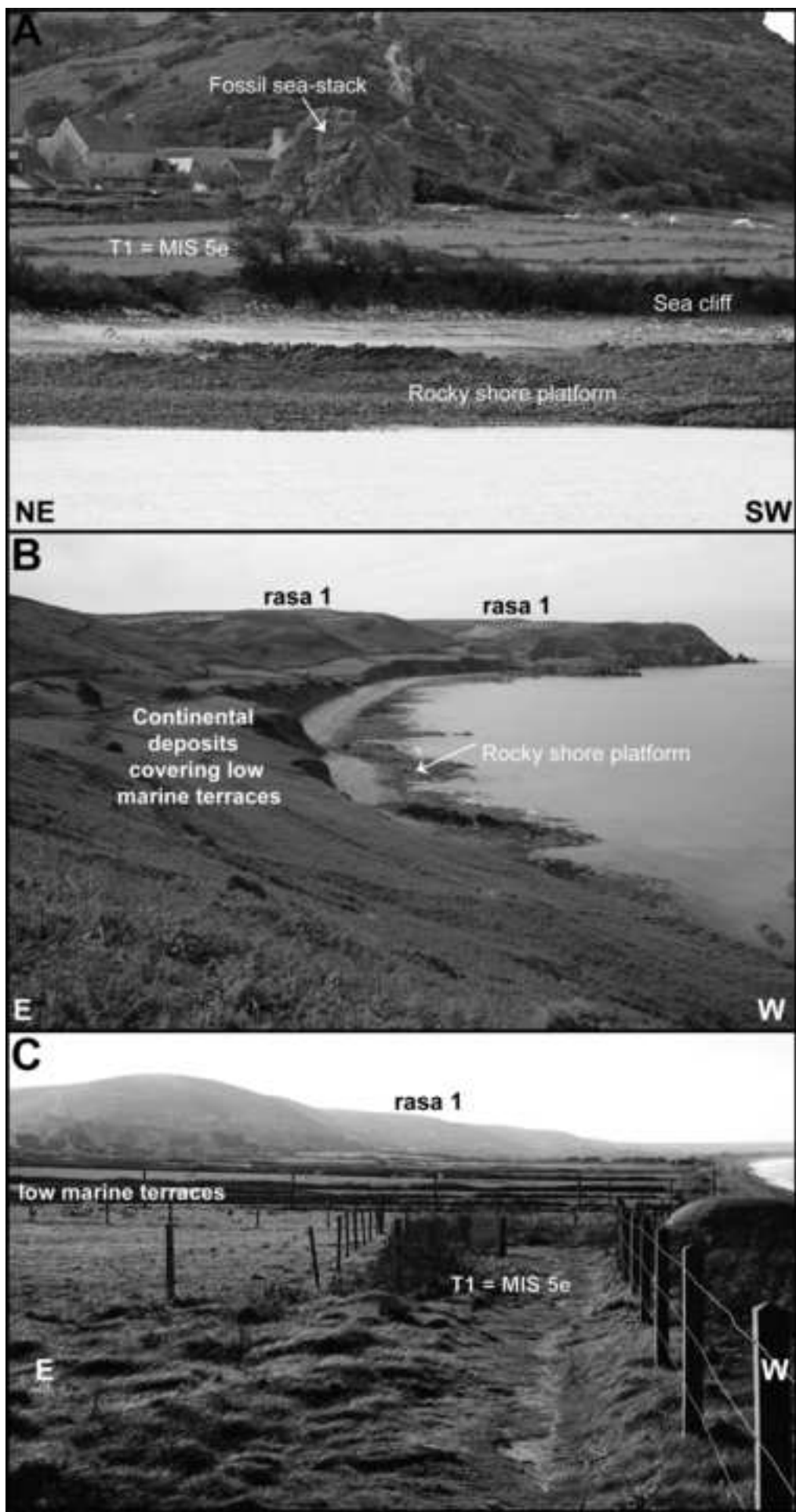


Figure 7 (Greyscale)

[Click here to download high resolution image](#)

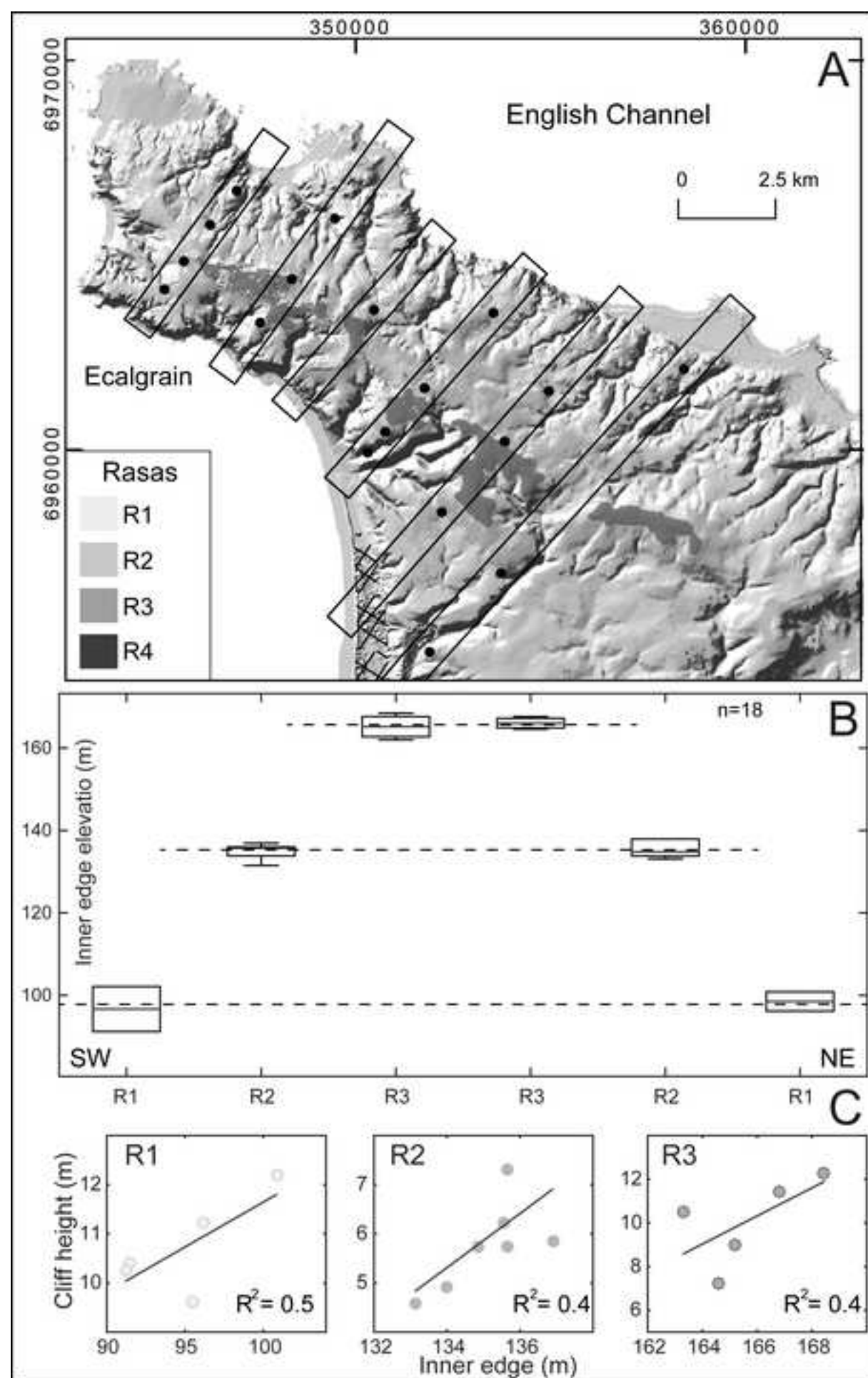


Figure 8 (Greyscale)

[Click here to download high resolution image](#)

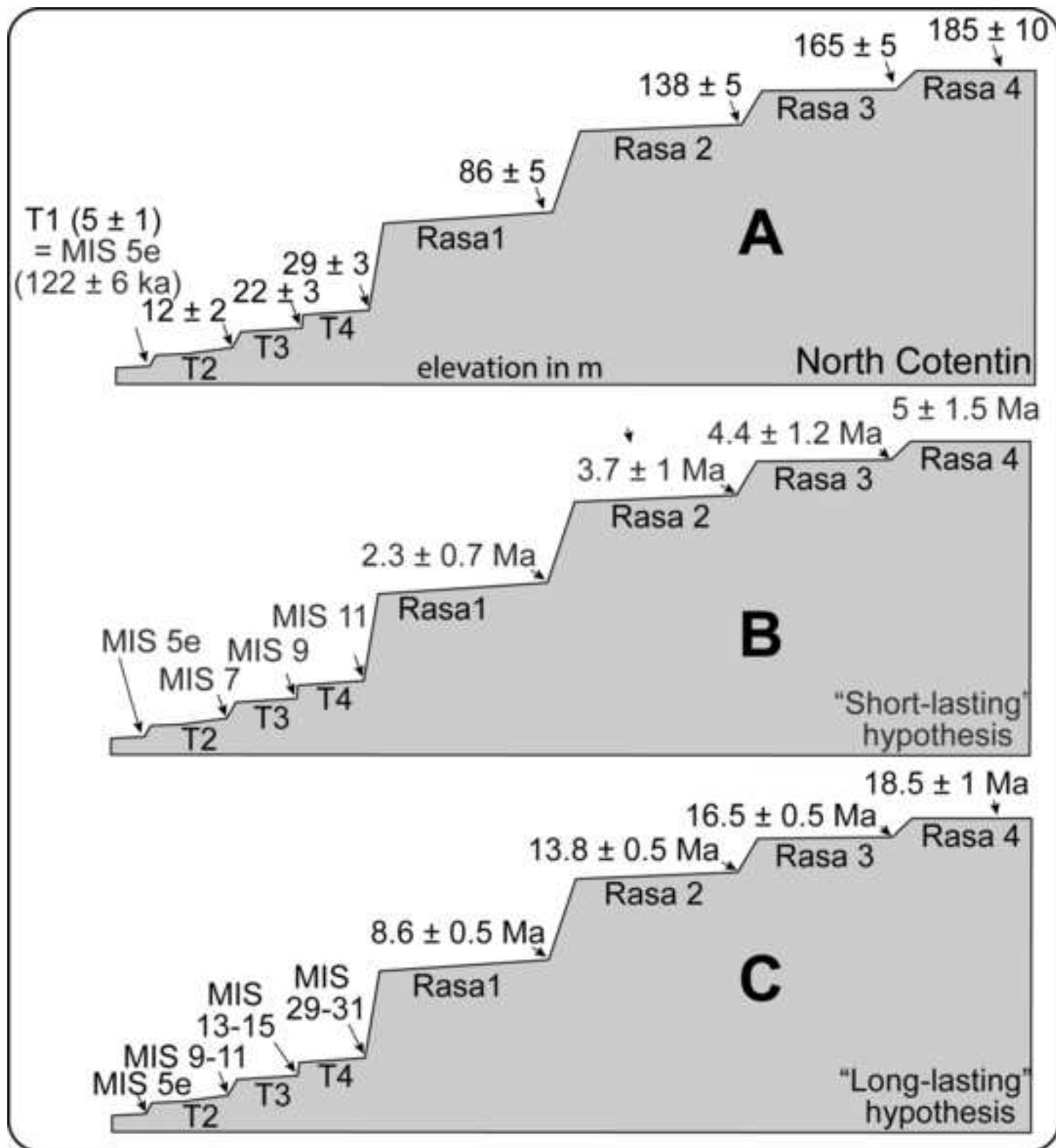
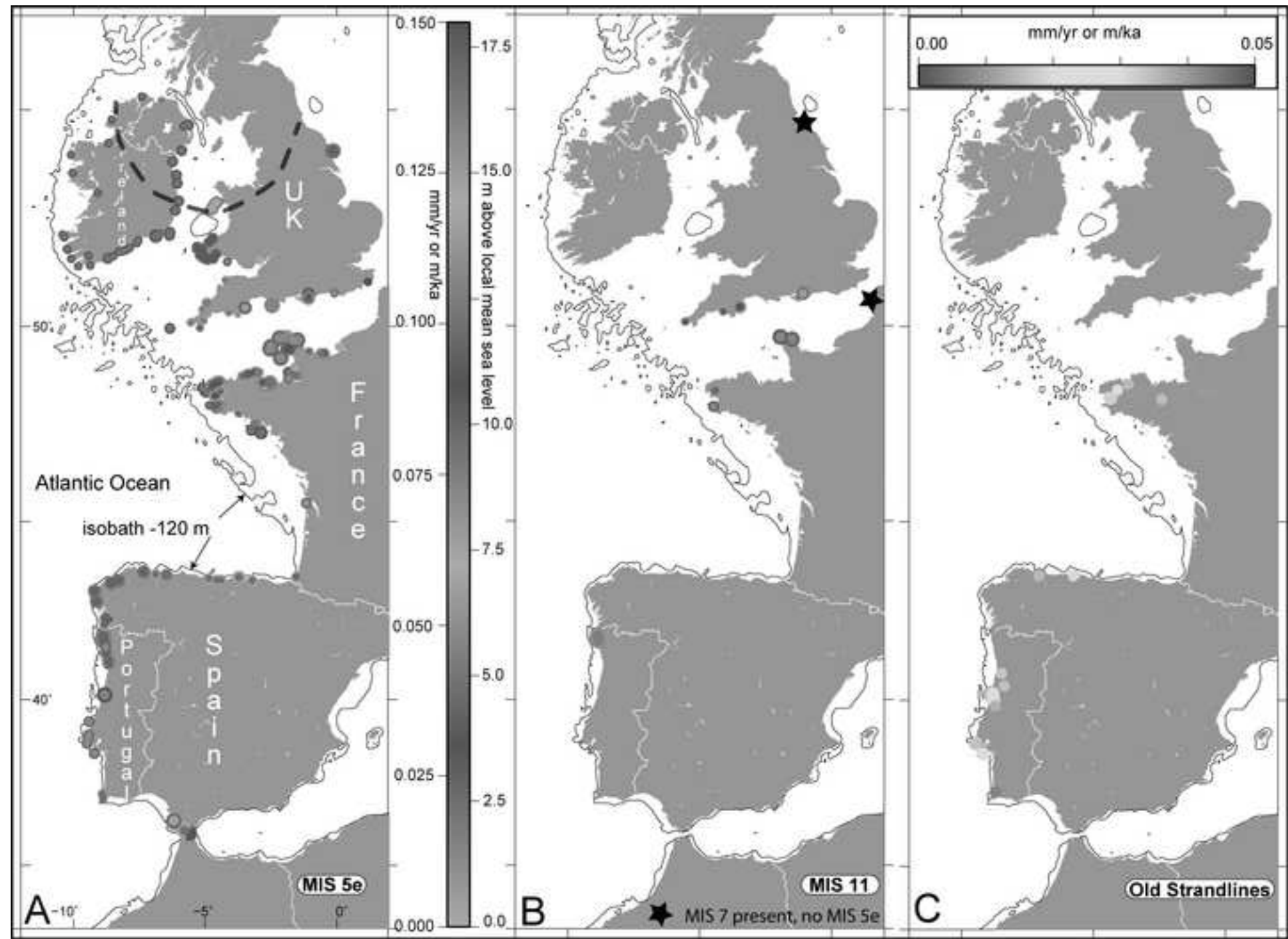


Figure (Greyscale) 10

[Click here to download high resolution image](#)



Edited supplementary material for online publication only

[Click here to download Supplementary material for online publication only: GEOMOR-6655R1 Edited Intro supp data Geom Atlan](#)

Supplementary material for online publication only

Click here to download Supplementary material for online publication only: Supp Table 1 W Europe MIS 5e MIS 11revised.xls

Supplementary material for online publication only

[Click here to download Supplementary material for online publication only: Supp Table 2 W Europe MIS 7.xls](#)

Supplementary material for online publication only

[Click here to download Supplementary material for online publication only: Supp Table 3 Old shoreline W Europe.xlsx](#)